International Journal of Engineering Research & Technology (IJERT)
ISSN: 2278-0181
Vol. 15 Issue 11 , November - 2026

Review on Back-Contact Engineering and Interface Physics in Lead-Free Perovskite Solar Cells

Ali AlMahmoud, Kaesar Alyamani, Omar AlAli, Hussein AlHussein
Ph.D. in Physics, Department of Physics, Faculty of Science, University of Aleppo
Assistant Professor, Department of Physics, Faculty of Science, Al -furat University
Ph.D. in Physics, Department of Physics, Faculty of Science, University of Aleppo
Ph.D. in Physics, Department of Physics, Faculty of Science, University of Aleppo

Abstract - The text presents a specialized scientific review titled "Review on Back-Contact Engineering and Interface Physics in Lead-Free Perovskite Solar Cells," which focuses on back-contact engineering and interface physics in lead-free perovskite solar cells—specifically those based on tin (Sn) as an alternative to toxic lead. The core problem and challenge: Although the efficiency of perovskite solar cells (PSCs) has advanced to exceed 26%, their reliance on lead poses environmental and health concerns. The alternative, Sn^{2+}, is prone to rapid oxidation into Sn^{4+}, which generates tin vacancies and leads to p-type self-doping; this, in turn, reduces the cell's open-circuit voltage (Voc) and its overall stability. Back-contact physics and charge transport: The review provides an in-depth examination of the physical mechanisms governing charge transport and injection at interfaces. The alignment between the work function of the back contact (ΦM) and the valence band energy (Ev) of the perovskite material is critical; a mismatch can lead to the formation of Schottky barriers that impede hole transport, resulting in S-shaped J-V curves and a significant reduction in the fill factor (FF). The text also addresses band alignment, ohmic contacts, the role of hole transport layers (HTLs), and methods for simulating device performance using software such as SCAPS-1D. Materials and stability challenges: The text discusses challenges related to the long-term stability of the materials. While noble metals—such as gold (Au) and platinum (Pt)—offer ideal work functions that ensure excellent charge extraction and high theoretical efficiencies, their high cost and potential for migration into the perovskite layer present significant structural challenges. In contrast, carbon and reduced graphene oxide (rGO) electrodes represent a promising, cost-effective alternative in terms of chemical stability and moisture resistance. However, controlling their porosity, ensuring uniform distribution, and minimizing interfacial defects—which often arise during manufacturing—remain significant challenges that require ongoing engineering improvements to achieve competitive experimental efficiencies.

Keywords - Lead-free perovskite solar cells (LF-PSCs), tin-based perovskites ($CsSnI_3$, $FASnI_3$), back-contact engineering, interface physics, work function (ΦM), simulation using SCAPS-1D software, carbon electrodes, hole transport layers (HTLs)

1. INTRODUCTION

The rapid development of solar energy over the past two decades reflects the growing demand for clean, reliable, and low-carbon energy sources. Concerns related to climate change, air pollution, energy security, and the gradual depletion of fossil-fuel resources have further intensified the search for sustainable photovoltaic technologies [1,2,4,5]. Silicon solar cells currently dominate the photovoltaic market because of their high efficiency, long-term stability, and well-established manufacturing infrastructure. Nevertheless, conventional silicon technology often requires high-temperature processing, high-purity materials, and relatively energy-intensive fabrication. These requirements have encouraged the development of emerging thin-film technologies that may offer simpler processing, lower material consumption, and reduced manufacturing costs [6-8].

Among these emerging technologies, perovskite solar cells (PSCs) have attracted exceptional scientific and industrial interest. Their power conversion efficiency (PCE) has increased from approximately 3.8% in the first reported devices to more than 26% in laboratory-scale single-junction cells within a relatively short period [9-14]. This rapid progress has placed PSCs among the leading candidates for next-generation photovoltaic applications. Their potential is not limited to single-junction solar cells. Perovskite materials are also being investigated for tandem devices, indoor photovoltaics, flexible and semitransparent modules,

(This work is licensed under a Creative Commons Attribution 4.0 International License.)

International Journal of Engineering Research & Technology (IJERT)
ISSN: 2278-0181
Vol. 15 Issue 11 , November - 2026

and lightweight power sources. These applications are enabled by the combination of strong optical absorption, compositional flexibility, and compatibility with low-temperature deposition processes. The outstanding photovoltaic performance of PSCs originates mainly from the favorable optoelectronic properties of halide perovskite absorbers. These materials generally exhibit high absorption coefficients, tunable bandgaps, relatively low exciton binding energies, and long carrier-diffusion lengths [15,20]. Consequently, a perovskite layer only a few hundred nanometers thick can absorb a substantial fraction of incident sunlight. Many perovskites also show relatively high carrier mobility and a certain degree of defect tolerance. In this context, defect tolerance refers to the ability of a material to accommodate some structural defects without generating a high density of deep electronic traps. Some defects may instead produce shallow states, which are less detrimental to charge transport. However, this tolerance is not unlimited, and excessive defect densities can still increase non-radiative recombination and reduce device performance [21,22].

The structural flexibility of halide perovskites provides an additional advantage. Their idealized structure is commonly represented by the formula ABX_3, where A is a monovalent organic or inorganic cation, *B* is typically a divalent metal cation, and X is a halide anion. Substitution at any of these sites can modify the bandgap, crystal stability, carrier concentration, defect chemistry, and energy-level alignment at the interfaces. This compositional flexibility allows perovskite absorbers to be tailored for different device architectures and operating conditions. However, the same structural flexibility can also introduce chemical and phase instabilities. Therefore, the advantages of perovskites must be considered together with the defects, ion migration, interfacial reactions, and environmental limitations that influence their long-term operation.

Despite the remarkable progress of PSCs, most high-efficiency devices still rely on lead-based absorbers, including methylammonium lead iodide ($MAPbI_3$), formamidinium lead iodide ($FAPbI_3$), and inorganic cesium lead halides [23,24]. These materials provide excellent optoelectronic properties, but the use of toxic lead raises important environmental and health concerns [25-28]. Lead release may occur during precursor preparation, device fabrication, operation under humid conditions, accidental module damage, or disposal. Encapsulation can reduce the possibility of lead leakage, but it cannot completely eliminate concerns related to large-scale manufacturing, module damage, and end-of-life management. These concerns have stimulated extensive research into lead-free and low-lead perovskite absorber materials.
Replacing lead is challenging because the alternative element must meet several requirements simultaneously. It must provide a suitable electronic structure, enable the formation of high-quality films, maintain controllable defect concentrations, and improve environmental compatibility [28-32]. Tin-based perovskites are among the promising alternatives because Sn^{2+} and Pb^{2+} have similar electronic configurations in the valence shell. Consequently, tin perovskites can exhibit relatively narrow direct energy gaps, strong optical absorption, and favorable charge carrier transport. Representative materials include $CsSnI_3$, $FASnI_3$, $MASnI_3$, $CsSnBr_3$, and mixed halide compounds such as $CsSn(I1{-}xBrx)_3$ [33-35]. However, the electronic similarity between Sn^{2+} and Pb^{2+} does not lead to equivalent chemical stability. Sn^{2+} oxidizes readily to Sn^{4+} in the presence of oxygen and moisture, and this process can be accelerated by thermal stress or unsuitable processing conditions. Oxidation is often associated with the formation of tin voids, VSn, which may induce strong p-type self-grafting [36-39]. A moderate concentration of holes may facilitate charge transport, but excessive self-doping increases charge carrier density in the dark and promotes non-radiative recombination. It can also reduce the depletion region width, increase voltage loss, and shorten charge carrier lifetime. These effects typically result in lower open-circuit voltage, reduced repeatability, and decreased operational stability. Therefore, the performance of tin-based solar cells cannot be evaluated based solely on the absorption band gap. Defect chemistry, oxidation control, in-cell and interfacial recombination, transport layer characteristics, and electrical connection geometry must all be considered [31, 37, 40].

1.1. CsSnI3as a Lead-Free Absorber

Among lead-free inorganic perovskites, $CsSnI_3$ has received considerable attention. It is a direct-bandgap semiconductor with a bandgap commonly reported near 1.3 eV, although the exact value depends on the crystal phase, fabrication conditions, film quality, and measurement technique [32,34,41]. This bandgap lies close to the range considered favorable for single-junction solar-energy conversion. CsSnI3also exhibits strong optical absorption and potentially favorable charge transport. In addition, its inorganic cesium cation can reduce some of the thermal instability associated with volatile organic cations [41,42].
The main challenge is that $CsSnI_3$ remains highly sensitive to oxidation and phase instability. Its structural and optoelectronic properties can change with temperature, ambient atmosphere, film morphology, vacuum conditions, and the chemical nature of adjacent layers. The formation of Sn4+and conductive degradation products can increase recombination and shorten the device lifetime [37-43]. Consequently, several strategies have been investigated, including additive engineering, controlled crystallization, inert-atmosphere

(This work is licensed under a Creative Commons Attribution 4.0 International License.)

International Journal of Engineering Research & Technology (IJERT)
ISSN: 2278-0181
Vol. 15 Issue 11 , November - 2026

processing, encapsulation, and interfacial passivation. These approaches can improve material stability, but they do not remove the need for careful contact design.

The back contact is particularly important because it determines how efficiently holes are extracted from the absorber and how strongly the rear interface contributes to recombination or degradation. An unsuitable contact can produce an extraction barrier, increase the series resistance, or promote chemical reactions with the perovskite. Since $CsSnI_3$combines an attractive bandgap with pronounced defect and contact-related challenges, it provides a useful reference system for comparing other lead-free absorbers [44-47]. Studies of $CsSnI_3$ can also provide transferable insights into work-function matching, interface-defect control, metal-induced degradation, and the relationship between contact chemistry and device stability.

1.2. Organic–Inorganic Tin Perovskites:

$FASnI_3$ and $MASnI_3$ Formamidinium tin iodide, $FASnI_3$, is one of the most widely investigated lead-free tin perovskites. It generally exhibits a direct bandgap of approximately 1.3–1.4 eV, strong absorption in the visible and near-infrared regions, and favorable charge-carrier transport properties [11-13]. Under appropriate processing conditions, the formamidinium cation can support the formation of a relatively stable perovskite structure [48,49]. These characteristics have enabled $FASnI_3$ to achieve some of the highest reported efficiencies among lead-free tin-based PSCs.

Nevertheless, the performance of $FASnI_3$ is still limited by Sn^{2+} oxidation, a high background hole concentration, and a substantial open-circuit voltage deficit. The interface between $FASnI_3$ and the hole-selective contact is especially significant. An excessive valence-band offset can cause hole accumulation at the interface, increase recombination, and produce non-ohmic current–voltage behavior [49,51]. This has motivated interest in carbon electrodes and hole-transport-layer-free structures. Such architectures may lower fabrication costs and reduce the chemical instability associated with some conventional organic hole-transport materials [50-52]. However, the advantages of carbon-based structures depend strongly on their work function, surface chemistry, contact resistance, morphology, and interfacial defect density. Thus, replacing a conventional HTL or metal electrode with carbon does not automatically guarantee better performance.

Methylammonium tin iodide, $MASnI_3$, is another important lead-free absorber. It has a narrow direct bandgap, generally reported between 1.2 and 1.4 eV, and can absorb a broad part of the solar spectrum [53,54]. $MASnI_3$ is often used as a reference material for organic–inorganic tin perovskites because its structural and optoelectronic characteristics are related to those of the extensively studied lead-based methylammonium perovskites. Although $MASnI_3$ can provide favorable charge transport, its stability is restricted by both tin oxidation and the limited thermal and chemical stability of the methylammonium cation [55,56]. The performance of $MASnI_3$ devices depends on the properties of the electron- and hole-transport layers, the density of interface defects, and the work function of the rear electrode. Metal contacts may diffuse into the absorber or react with iodine-containing species, while low-work-function contacts may create an unfavorable barrier to hole extraction. Therefore, contact selection requires a compromise between electrical conductivity, energy-level alignment, chemical compatibility, thermal stability, and cost [57-59]. This issue is important for lead-free devices because the contact must support charge extraction without accelerating the degradation processes that already limit tin-based absorbers

1.3. Tin Perovskites Containing Bromide and Mixed Halides

Halide substitution is a practical method for tuning the optical and electronic properties of tin perovskites. Partial or complete iodine substitution in $CsSnI_3$ with bromide yields $CsSn(I_{1-x})$
$(Brx)_3$ and the final compound $CsSnBr_3$. In general, increasing the bromide content leads to a wider energy gap, while mixed halide compositions exhibit intermediate values [60, 63]. This tunability can be useful for controlling the balance between photocurrent and open-circuit voltage. A wider energy gap may reduce the maximum photocurrent in a single-junction device, but it may increase the achievable voltage if non-radiative recombination is suppressed. Wide bandgap structures may also be suitable for top cells in tandem structures or for applications requiring spectral matching. The introduction of bromide not only affects the bandgap but may also alter crystal stability, defect formation energies, charge carrier concentration, and energy level alignment at the interfaces [46, 61–65]. Consequently, a back conductor that performs well with $CsSnI_3$ may not be ideal for CsSnBr3 or a mixed halide structure. Therefore, the structure coefficient x in $CsSn(I_{1-x}Br_x)_3$ should be evaluated. This relationship makes mixed tin halide perovskites useful systems for investigating how the structure of the adsorbent affects back-surface charge extraction.

However, the advantages of halide blending are accompanied by practical limitations. Halide blended perovskites may undergo halide dissociation under the influence of illumination or an electric field. This process can generate regions with different energy gaps, leading to localized fluctuations in electrical potential and additional recombination pathways. Therefore, the theoretical advantage of the ability to tune

(This work is licensed under a Creative Commons Attribution 4.0 International License.)

International Journal of Engineering Research & Technology (IJERT)
ISSN: 2278-0181
Vol. 15 Issue 11 , November - 2026

the energy gap must be considered alongside ion migration, phase separation, and interface instability [66-77]. These effects can alter the alignment of effective energy bands during operation and may reduce the reliability of contact optimization based solely on the base material parameters.

2. FUNDAMENTALS OF BACK-CONTACT AND INTERFACE PHYSICS IN PSCS

2.1. Energetics and Band Alignment at the Rear Interface

The rear interface critically influences hole extraction, recombination losses, and series resistance (Rs) in perovskite solar cells [78,79]. A primary criterion for contact evaluation is the electrode work function ($\Phi_M = E_{vac} - E_F$). For p-type perovskites, high-Φ_M materials are generally favored to minimize the energetic barrier between the electrode Fermi level and the valence-band maximum (VBM) of the absorber or hole-transport layer (HTL) [78–80]. Favorable alignment establishes an ohmic-like contact, facilitating hole collection, improving the fill factor (FF), and reducing voltage deficits (Voc losses) [79–81]. Conversely, an energetic mismatch induces a Schottky-type barrier, impeding hole extraction and promoting carrier accumulation near the rear contact [80,81]. This accumulation enhances trap-assisted recombination and often manifests as an S-shaped J_V curve or current–voltage rollover under operating conditions [80,81]. However, vacuum work-function values offer only an initial approximation. In real devices, effective band alignment is substantially modified by interface dipoles, Fermi-level pinning via surface states, interdiffusion, and interfacial chemical reactions especially under thermal or illumination stress [84,85]. The presence of an HTL further modifies these energetic constraints. In HTL-based architectures, the electrode work function must match the highest occupied molecular orbital (HOMO) or V_{BM} of the transport layer, which simultaneously blocks electrons and protects the absorber from direct chemical degradation [78,82,83]. In HTL-free configurations, the electrode contacts the perovskite directly, making band alignment, surface passivation, and chemical stability far more critical [52,88]. This distinction is vital for tin-based perovskites, where Sn^{2+} oxidation creates tin vacancies (V_{Sn}) and heavy p-type self-doping [36–40]. Such doping alters the depletion region and band bending, changing contact requirements compared to stoichiometric absorbers [40,81]. Furthermore, the work function of non-metallic electrodes—such as carbon paste, graphite, and reduced graphene oxide (rGO)—varies significantly with synthesis routes, degree of reduction, oxygen-containing functional groups, and porosity [86–89]. Consequently, contact optimization cannot rely on bulk nominal values alone. Numerical tools like SCAPS-1D allow decoupled analysis of Φ_M, interface-defect density, and contact resistance [90–92]. In summary, selecting an optimal back contact requires an integrated assessment of work-function matching, interfacial charge selectivity, defect dynamics, and chemical stability rather than simple bulk conductivity [78–81,84–92].

3. LEAD-FREE AND TIN-BASED PEROVSKITES AND BACK CONTACT ENGINEERING

Tin-based perovskites are among the most studied lead-free absorbers due to their suitable band gap, strong light absorption, and relatively good charge transfer [100-102]. Materials such as $FASnI_3$, $MASnI_3$, and $CsSnI_3$ have attracted considerable attention as potential alternatives to lead-based perovskites [100, 101]. However, their practical application remains limited due to several stability and defect issues. The most significant of these is the easy oxidation of Sn^{2+} to Sn^{4+}, which generates numerous defects and greatly increases p-type self-grafting [36-40, 100-102]. This background deficiency directly impacts back contact. Because tin-based perovskites have a high density of voids and free holes, the back-end interface becomes highly sensitive to any additional barrier or recombination site [40, 100–103]. A contact that functions efficiently in a lead-based device may not be as effective here. In these systems, the back-end contact geometry not only efficiently extracts holes but also minimizes additional loss channels in an inherently defective absorber material [101–103]. Carbon electrodes have been extensively studied in tin-based perovskite solar cells due to their low cost, chemical stability, and compatibility with low-temperature manufacturing processes [86–89, 100–104]. They also avoid the problem of metal diffusion and halide-induced corrosion, which often occurs with noble metals [98, 99]. However, carbon is not a perfect solution. Its work function, conductivity, and interfacial quality depend heavily on its composition, porosity, binder content, and manufacturing method [86-89]. Consequently, performance can vary considerably from one report to another, even when the device structure appears similar. Reduced graphene oxide (rGO) has been investigated as a background contact material or intermediate layer due to its ability to combine better conductivity with some degree of work function tunability [86-89, 104, 105]. In some studies, rGO improves hole extraction and helps reduce recombination at the interface. In other studies, however, the benefit is less due to less-than-ideal layer quality, reduction level, and film continuity. This suggests that rGO should not be treated as an invariant material property, but rather its actual role depends on how it is processed and how well it contacts the perovskite or transport layer [86-89, 104, 105]. Another important consideration is the use of hole-transport-layer (HTL)-free structures. These devices are characterized by their simplified installation and lower cost, but they make the back interface more critical [102-105]. Without a dedicated

(This work is licensed under a Creative Commons Attribution 4.0 International License.)

International Journal of Engineering Research & Technology (IJERT)
ISSN: 2278-0181
Vol. 15 Issue 11 , November - 2026

hole-transfer layer, the back electrode must directly handle charge accumulation while preventing unwanted recombination. This places greater emphasis on energy band alignment, surface passivation, and chemical compatibility. In tin-based perovskites, where the absorber is unstable and defect-rich, this challenge becomes even more pronounced [40, 101-105]. Several studies have shown that device performance can be improved by optimizing the back conductor in conjunction with absorber installation and interface treatment [100-105]. For example, reducing oxidation, controlling void formation, and improving surface passivation can make the back conductor more efficient. This means that the back electrode should not be studied in isolation, as its behavior depends on the absorber's chemical composition, the quality of the interface, and the overall device design [101-105]. In general, lead-free and tin-based perovskites are promising, but their back-conducting engineering remains a major obstacle. The primary challenge is combining highly efficient hole extraction, a low recombination rate, and strong chemical stability. Carbon and reduced graphene oxide (rGO) are attractive options due to their stability and low cost, but their actual performance depends on the quality of the treated interface. For this reason, the literature should be read critically, paying attention to both material selection and interface engineering strategy [86-89, 98-105].

3.1. Carbon and Carbon Electrodes in Tin Perovskite Solar Cells

Carbon electrodes have become one of the most common back-contact compositions in tin perovskite solar cells [106–109]. Their popularity stems from a simple combination of low cost, chemical stability, and compatibility with low-temperature manufacturing processes. Unlike precious metals, carbon does not readily diffuse into the perovskite layer and does not react strongly with halide compounds under normal operating conditions [98, 99, 106]. This makes it an attractive choice for devices requiring better long-term stability and lower manufacturing costs. This characteristic is particularly important in tin perovskite, as these adsorbent materials are already susceptible to oxidation, defect formation, and self-grafting [36–40, 100–102]. Metallic contact may introduce another degradation pathway, while carbon acts as a more inert back electrode. For this reason, many studies use carbon as a current collector and as a protective back contact layer [106-109]. In some device designs, carbon simplifies the structure by eliminating the need for a separate hole-transfer layer. However, carbon is not an ideal electrode. Its performance depends heavily on its composition, particle size, porosity, binder content, and printing or deposition method [86-89, 106-109]. Two carbon electrodes may appear structurally similar but behave differently in a device. This is because carbon paste is not a single material with constant properties. Its conductivity and occupational function change with the manufacturing process, which directly affects hole extraction and contact resistance [86-89]. If the contact is highly resistant or highly porous, charge carriers may accumulate at the back surface and aggregate before collection. Another limitation is the quality of the interfacial contact. Carbon electrodes often form mechanically stable contacts, but electrical contact with the perovskite or transport layer is not always ideal [106-109]. If the surface is rough, imperfect, or poorly passivated, back contact may result in additional recombination losses. In this case, the stability advantage of carbon may come at the cost of reduced efficiency. Thus, the main challenge is maintaining contact stability without sacrificing charge extraction. Studies also indicate that carbon improves performance when the interface is carefully engineered. Surface passivation, control of perovskite crystallinity, and optimization of layer density can all contribute to improving the efficiency of carbon contacts [106-110]. This means that the electrode alone is insufficient. Device performance depends on all its components, especially the quality of the back interface and the density of defects in the adsorbent material. Therefore, carbon-based electrodes are seen as a practical compromise. They are generally more stable and less expensive than metallic contacts, but they may also introduce transport limitations if the interface is not well-designed. For tin perovskites, where stability is already a major issue, this compromise is often acceptable. However, studies should not overestimate carbon as a panacea. Its success depends on how well it is integrated into the device, not just on the material itself [86-89, 106-110].

3.2. Reduced Graphene Oxide (rGO) as a Back Contact Layer

Extensive research is being conducted on reduced graphene oxide (rGO) as a replacement or modifier for back contact layers in tin-based perovskite solar cells [111-114]. Compared to conventional carbon pastes, rGO exhibits higher self-charge carrier mobility, good mechanical flexibility, and tunable functional properties [86, 88, 111]. Its two-dimensional sheet structure can also act as a physical barrier against moisture and oxygen, helping to slow the oxidation of Sn^{2+} to Sn^{4+} in the underlying adsorbent [112, 113]. One of the most important advantages of rGO is the tunability of its electronic properties. By changing the reduction method—whether thermal, chemical, or electrochemical—the sp2 ratio of carbon to oxygen-containing functional groups (such as hydroxyl, epoxy, and carboxyl groups) can be controlled [86, 87, 114]. This leads to a direct modulation of both the electrical conductivity and the work function, which typically range

(This work is licensed under a Creative Commons Attribution 4.0 International License.)

International Journal of Engineering Research & Technology (IJERT)
ISSN: 2278-0181
Vol. 15 Issue 11 , November - 2026

between 4.4 and 5.1 eV [86, 88]. When properly tuned, the Fermi level of reduced graphene oxide (rGO) more closely matches the valence band of tin perovskite, reducing the hole extraction barrier and lowering the series resistance compared to standard graphite pastes [111, 114]. However, reduced graphene oxide is not without its practical drawbacks. Incomplete reduction leaves behind excess oxygen defects, which act as charge carrier traps and reduce the overall conductivity [87, 115]. On the other hand, excessive reduction can cause sheet re-cluttering due to strong van der Waals forces, resulting in poor film uniformity, micropore formation, and reduced coverage on the perovskite layer [113, 115]. If the r/educed graphene oxide (rGO) film is disconnected, local contact resistance increases and switching pathways may form, reducing both the fill factor and the open-circuit voltage [111, 113]. Due to these trade-offs, rGO is rarely used as a standalone thick electrode in high-performance devices. Instead, studies show better results when used as an ultrathin dielectric layer at the interface or when blended with carbon pastes as a conductive additive [112, 114, 116]. In composite electrodes (such as carbon/rGO blends), rGO fills the gaps between larger graphite or carbon black particles, enabling faster hole permeability pathways while maintaining the chemical stability and low cost of carbon [114, 116]. In summary, rGO is a promising material for back-contact engineering in lead-free tin perovskites, but its benefits are highly dependent on manufacturing quality. It should not be treated as a single, homogeneous material. Its effectiveness depends on finding the optimal balance between the degree of reduction, layer dispersion, and film shape at the back interface [86-88, 111-116].

3.3. Critical Comparison of Metallic and Carbon/Reduced Graphene Oxide Conductors

The choice of back conductor is not a minor detail in tin-based perovskite solar cells, as it can significantly affect charge extraction, recombination loss, operational stability, and manufacturing cost. For this reason, it is useful to compare conventional metal conductors with carbon electrodes and reduced graphene oxide from a practical, rather than solely a materials chemistry, perspective. Noble metals, such as gold, are often attractive due to their high conductivity and relatively stable electrical conductivity. In many cases, these metals provide good hole extraction when the work function is reasonably compatible with the adsorbent material [117-119]. However, this advantage comes with clear limitations. Gold is expensive, and its use is unsuitable for large-scale, low-cost photovoltaic applications. More importantly, metal atoms may diffuse into the perovskite layer during operation or thermal stress, especially when the interface is defective or poorly sealed [118, 119]. In lead-free tin perovskites, where the absorber already suffers from defect formation and oxidation, this additional disturbance is a real concern. Other metals such as silver, copper, aluminum, nickel, molybdenum, tungsten, chromium, and iron have been explored as back-connectors [120–124]. Some of these metals are cheaper than gold, but each has its drawbacks. Silver and copper may suffer from halide corrosion or interfacial reactions. Aluminum may oxidize rapidly and form an undesirable barrier. Transition metals can offer useful functionalities and lower costs, but their compatibility depends heavily on the interface chemistry, layer quality, and operating environment [120–124]. In short, a low-cost metal is not necessarily a good back-connector. Carbon electrodes avoid some of these problems. They are generally more chemically stable, less prone to metal migration, and easier to incorporate into low-temperature fabrication methods [106-110, 121-124]. This makes them particularly attractive for tin perovskites, where the back face must remain stable under defect-rich and oxidation-prone conditions. Their main weakness lies not in chemical instability, but in contact quality. If the carbon layer is porous, uncompressed, or poorly bonded to the adsorbent, the device may lose efficiency due to increased series resistance and increased recombination at the interface. Reduced graphene oxide (rGO) falls somewhere between a conventional carbon electrode and an enhanced conductive layer. It improves conductivity, modifies the work function, and helps establish better contact at the back face [111-116]. However, these benefits are again process-dependent. A poorly reduced or poorly distributed rGO layer may behave worse than expected. Therefore, rGO should be considered a contact engineering tool, not a universal replacement for metals. The key point is simple: the best back contact is not necessarily the one with the highest conductivity, nor is it simply the cheapest. It is the material that combines a suitable work function, low recombination at the interface, chemical compatibility, and long-term stability. For lead-free, tin-based perovskite solar cells, carbon and reduced graphene oxide (rGO) are often more realistic than precious metals, but their performance still depends on how well the back interface is engineered [106-124].

3.4. SCAPS-1D as a Back Contact Design Tool

The SCAPS-1D software has become one of the most practical tools for studying thin-film solar cells prior to fabrication [125-128]. It enables researchers to test how the properties of the absorber material, defect density, interfacial states, contact work function, and transport layer parameters affect device performance. This software is particularly useful in back contact engineering, as the back interface is often difficult to isolate experimentally. SCAPS-1D helps to isolate the effect of resistivity in lead-free perovskite solar cells and surface defect loss. This is a critical point for lead-free and tin-based perovskite solar cells. These devices

(This work is licensed under a Creative Commons Attribution 4.0 International License.)

International Journal of Engineering Research & Technology (IJERT)
ISSN: 2278-0181
Vol. 15 Issue 11 , November - 2026

are highly affected by oxidation of tin(II) ions (Sn^{2+}), tin voids, and self-doping [36-40, 100-102]. Consequently, back contact can help to efficiently collect holes or increase recombination if the compatibility is poor. The SCAPS-1D software allows for the study of how changes in the work function, defect density, and contact selectivity affect voltage (Voc), short-circuit current density (Jsc), fill factor (F_F), and power conversion efficiency [125-128]. This provides a clearer picture of physically reasonable versus unreasonable contact designs. Another advantage of SCAPS-1D is its ability to evaluate different device configurations under the same assumptions. For example, noble metal contacts, carbon electrodes, and rGO-modified contacts can be compared while keeping the absorption and transport layers unchanged. This makes the comparison more consistent. It also helps determine whether performance improvements result from improved energy band alignment, reduced recombination, or simply lower series resistance. Of course, SCAPS-1D does not replace experimentation. The model's reliability depends on the accuracy of its inputs. Real-world interfaces may exhibit roughness, chemical interactions, diffusion, and irregular defects that are difficult to fully represent in one-dimensional simulations. Nevertheless, SCAPS-1D remains valuable because it provides a controlled method for testing design ideas and narrowing down research prior to fabrication [125-132].

4.2. Carbon Back Contacts in Tin-Based Lead-Free Perovskite Solar Cells

Carbon electrodes have emerged as promising low-cost alternatives to noble-metal contacts in tin-based lead-free perovskite solar cells (PSCs), primarily because of their chemical stability, low material cost, and reduced susceptibility to metal-ion diffusion and halide-induced corrosion. Nevertheless, the reported performance of carbon-contacted tin perovskite devices varies considerably, indicating that the performance of the carbon electrode cannot be evaluated independently of the absorber composition, crystallization method, and quality of the rear interface. Tsai et al. investigated mesoscopic carbon-electrode solar cells based on hybrid formamidinium/2-hydroxyethylammonium tin iodide perovskites, $HEA_xFA_{1-x}SnI_3$, and identified $HEA_{0.4}FA_{0.6}SnI_3$ as the optimum composition. Using a solvent-extraction process and 3% $EDAI_2$, the resulting fresh device achieved a power conversion efficiency (PCE) of 3.7%, with a V_{oc} of 383 mV, a J_{sc} of 17.20 mA cm^{-2}, and a fill factor (F_F) of 0.56. After 340 h of storage in a glovebox, the device exhibited a PCE of 3.9%. These results demonstrate that carbon electrodes can function effectively in tin-based devices; however, the relatively low V_{oc} indicates substantial voltage losses, which are likely associated with tin vacancies, p-type self-doping, and interfacial recombination. Importantly, the observed improvement cannot be attributed to the carbon electrode alone because the study simultaneously modified the cation composition, crystallization route, and additive concentration.[133, 134], A related strategy was demonstrated using mixed-halide or superhalide-engineered tin perovskites. Rameez et al. developed $FASnI_{3-x}(BF_4)_x$ for mesoscopic carbon-based solar cells. The optimized composition, $FASnI(BF_4)_2$, produced a PCE of 1.3%, compared with 0.7% for the $FASnI_3$ reference device, corresponding to an improvement of approximately 72%. Despite this relative enhancement, the absolute efficiency remained low. The improvement was attributed to the suppression of Sn^{4+} formation and a reduction in trap-assisted recombination. This comparison highlights the strong influence of absorber chemistry on the performance of carbon-contacted devices. However, because the incorporation of BF^{4-} was not independently separated from the effect of the carbon electrode, the study does not provide direct evidence of the intrinsic advantage of carbon as a rear contact. The role of precursor chemistry was also examined in tin-rich mixed-halide perovskites incorporated into mesoscopic solar cells with carbon counter electrodes. In particular, the effect of $SnCl_2$ in the precursor and perovskite formation process demonstrated that precursor composition and electrode characteristics must be considered together. Variations in the amount of $SnCl_2$ can significantly influence defect chemistry, crystallization behavior, and carrier density within the absorber. Consequently, even when the carbon electrode remains chemically stable, the resulting device may still experience substantial bulk and interfacial recombination. This work is therefore relevant to the early development of carbon-contacted tin devices, although it should not be interpreted as direct evidence that carbon outperforms noble-metal contacts because a controlled electrode-to-electrode comparison under identical device conditions was not provided. Further evidence for the importance of absorber engineering was obtained from $FASnI_{3-x}(SCN)_x$ carbon-electrode solar cells. The best unoptimized $FASnI(SCN)_2$ device achieved a PCE of 2.4%, compared with 0.9% for the $FASnI_3$ reference. Following additional treatment with PEAI and $EDAI_2$, the device reached a J_sc of 20.17 mA cm^{-2}, a V_oc of 322 mV, an FF of 0.574, and a PCE of 3.7%. The incorporation of the pseudohalide was reported to suppress Sn^{2+} oxidation, reduce trap-assisted recombination, and enhance resistance to ambient degradation. Nevertheless, the simultaneous use of SCN^{1-}, PEAI, and $EDAI_2$ makes it difficult to identify which modification was primarily responsible for the improvement. Moreover, the relatively low Voc indicates that significant bulk and interfacial voltage losses remained unresolved. More recently, a doctor-bladed carbon electrode was combined with SnF_2–TMAB passivation in $FASnI_3$ solar cells employing NiO as the hole-transport layer. The resulting device achieved a reported PCE of up to 11.17%, while unencapsulated devices retained more than 70% of their initial

(This work is licensed under a Creative Commons Attribution 4.0 International License.)

International Journal of Engineering Research & Technology (IJERT)
ISSN: 2278-0181
Vol. 15 Issue 11 , November - 2026

performance for over 45 h in air and 75 h in nitrogen. This represents a substantial improvement compared with earlier carbon-electrode tin perovskite devices and demonstrates the practical potential of scalable carbon deposition techniques. However, the high efficiency cannot be assigned to the carbon electrode alone, since the device architecture incorporated several additional performance-enhancing strategies, including SnF_2–TMAB passivation, NiO-assisted hole extraction, improved grain protection, and suppression of Sn^{2+}oxidation. In addition, the reported stability duration is still limited compared with long-term maximum-power-point testing. The study therefore demonstrates a promising combined strategy rather than a fully isolated evaluation of the carbon rear contact. Overall, these studies support the use of carbon as a chemically stable and potentially scalable rear-contact material for tin-based lead-free perovskite solar cells. However, they also show that carbon does not solve the main limitations of tin perovskites by itself. Its benefit is mainly related to reduced metal-related degradation, while its limitations include relatively high contact resistance, surface roughness, porosity, and incomplete physical contact with the perovskite or hole-transport layer. The final device performance is therefore determined by the combined effects of carbon processing, work-function alignment, absorber defect density, interfacial recombination, and chemical stability. A key limitation of the current literature is the lack of controlled comparisons between carbon and noble-metal contacts using the same absorber, transport layers, and processing conditions. Most studies improve the absorber or interface at the same time as they introduce the carbon electrode. As a result, the independent effect of the rear contact remains unclear. Future studies should report the work function, contact resistance, surface morphology, interfacial defect density, and stability under identical testing conditions. Such data would allow the role of the carbon electrode to be separated from the effects of bulk passivation and absorber engineering.

Tsai et al. (2018) ,[134],fabricated tin-based, mesoscopic, hole-transport-layer-free perovskite solar cells (PSCs) using screen-printed carbon electrodes (FTO/c-TiO_2/mp-TiO_2/mp-Al_2O_3/Carbon), incorporating the material $HEA_{0.4}FA_{0.6}SnI_3$ with 3% $EDAI_2$ additives. The device achieved an efficiency of 3.7% (Voc = 383 mV, Jsc = 17.20 mA/cm², F_F = 0.56), attributed to a deeper valence band alignment (-5.29 eV) and longer charge-carrier lifetimes (1.7 ns). However, the carbon contact failed to address the significant open-circuit voltage deficit (Voc < 400 mV for a bandgap of Eg = 1.53 eV), as illustrated in Figures (1-a, 1-b), indicating persistent interfacial recombination; meanwhile, the reported stability (approximately 340 hours inside a glovebox) reflects the inertness of the electrode encapsulation rather than true operational photostability.[134].

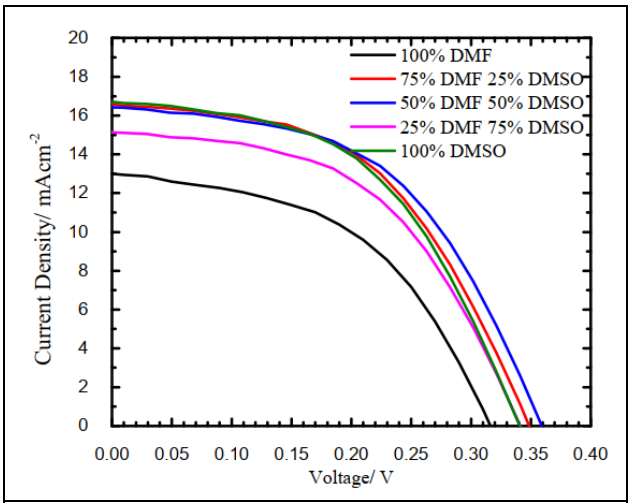


Figure 1.a . Photovoltaic (PV) performance of HEAI 40 % devices fabricated with the solvent extraction (SE) method with co-solvent DMF/DMSO at varied ratio.

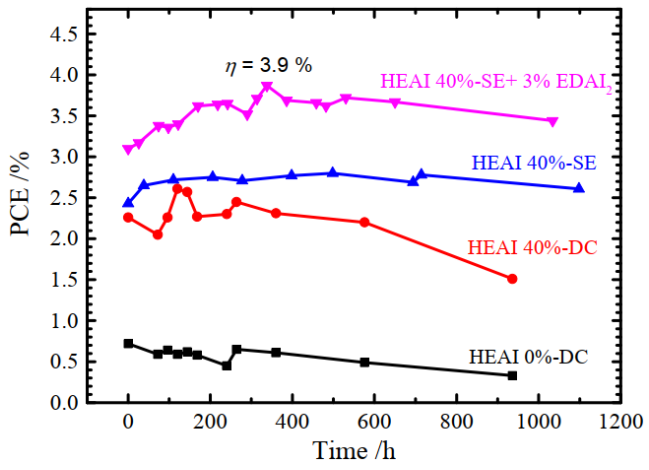


Figure 1.b. Efficiency stability profiles of HEAI 0% and HEAI 40% devices with different methods as a function of storage period.

The study conducted by Rameez et al. (2020) , As shown in Figure (2,a,b),investigated the substitution of iodide with the superhalide pseudohalogen tetrafluoroborate (BF^{4-}) in HTL-free monolithic carbon-based mesoscopic solar cells (FTO/c-TiO_2/mp-TiO_2/mp-Al_2O_3/Carbon) by developing $FASnI(BF_4)_2$ (FSB). The incorporation of BF^{4-} shifted the valence band maximum (E_{VB}) from −4.92 eV in pristine $FASnI_3$ to −5.18 eV, thereby improving the energetic alignment with the 15 μm printed carbon cathode and suppressing Sn^{2+} oxidation. Consequently, the champion device PCE increased from 0.70% to 1.3% (J_{SC} = 20.2 mA cm^{-2}, V_oc = 225 mV, FF = 0.34), accompanied by a reduction in charge-transfer resistance (Rct = 10.24 Ω) and an

(This work is licensed under a Creative Commons Attribution 4.0 International License.)

International Journal of Engineering Research & Technology (IJERT)
ISSN: 2278-0181
Vol. 15 Issue 11 , November - 2026

increase in recombination resistance (Rrec = 365.0 Ω). Nevertheless, the devices exhibited a very low fill factor (FF ≈ 0.32–0.34) and substantial series resistance (Rs = 51.35 Ω), highlighting persistent interfacial charge-extraction limitations within the thick mesoporous alumina/carbon architecture and incomplete suppression of interfacial defects.[135].

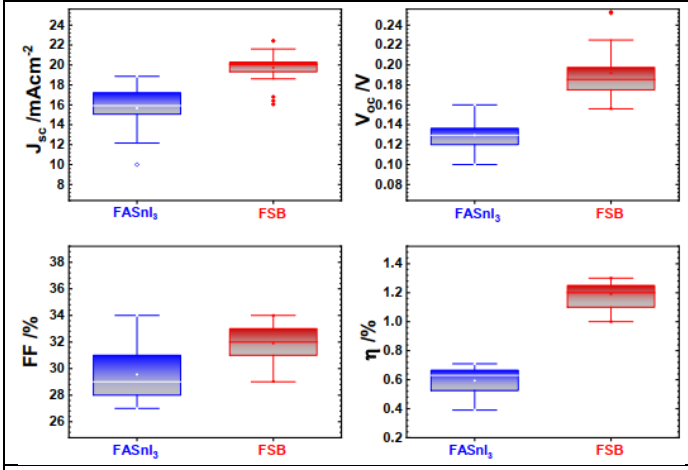


Figure 2.a. Statistical distributions of photovoltaic performance parameters for 20 devices prepared under the same conditions, for both FASnI3 and FSB devices.

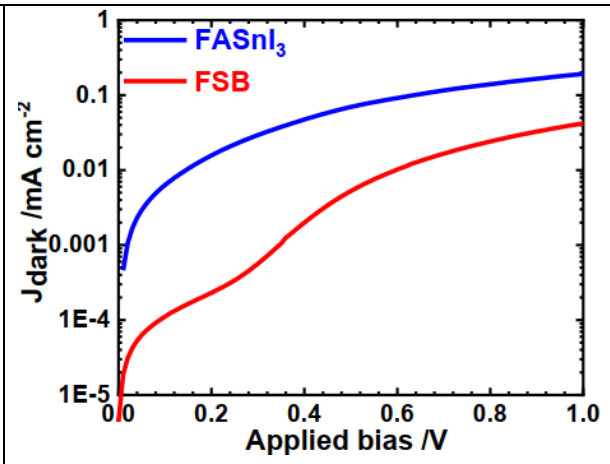


Figure 2.b. Dark J-V curves (semilog plot, cell area: 0.09 cm2) of the carbon-based FASnI3 and FSB perovskite solar cells as fabricated

The study conducted by Ramiz et al. (2020)[136]. introduced the thiocyanate ion (SCN^-) a pseudohalide and the bulky phenethylammonium cation (PEA^+) into monolithic, hole-transport-layer (HTL)-free mesoscopic carbon-based devices (with the architecture: FTO/c-TiO_2/mp-TiO_2/mp-Al_2O_3/Carbon), while incorporating a nickel oxide (NiO_x) interlayer. Integrating these components shifted the valence band maximum from -5.21 eV to -5.42 eV in the $PEA_{0.1}FA_{0.9}SnI(SCN)_2$ composition, thereby providing more favorable energy alignment with the printed carbon back electrode. Further optimization using 5% $EDAI_2$ (sample P10E5), combined with a solvent extraction technique, boosted device efficiency to 3.7% (with values of Voc = 322 mV, Jsc = 20.17 mA/cm², and F_F = 0.57). As shown in Figure (3,4), This was accompanied by a notable increase in recombination resistance (Rrec) from 111.8 Ω to 566.1 Ω and an extension of the charge-carrier lifetime (τ_{PL}) to 5.94 ns. Despite these improvements, the open-circuit voltage (Voc) remained limited to approximately 0.32 V, even after extensive passivation of both the bulk structure and the surfaces. This indicates that non-radiative recombination at the back carbon interface and the resulting severe voltage deficit remains a major obstacle in tin-based carbon cell structures. [136].

(This work is licensed under a Creative Commons Attribution 4.0 International License.)

International Journal of Engineering Research & Technology (IJERT)
ISSN: 2278-0181
Vol. 15 Issue 11 , November - 2026

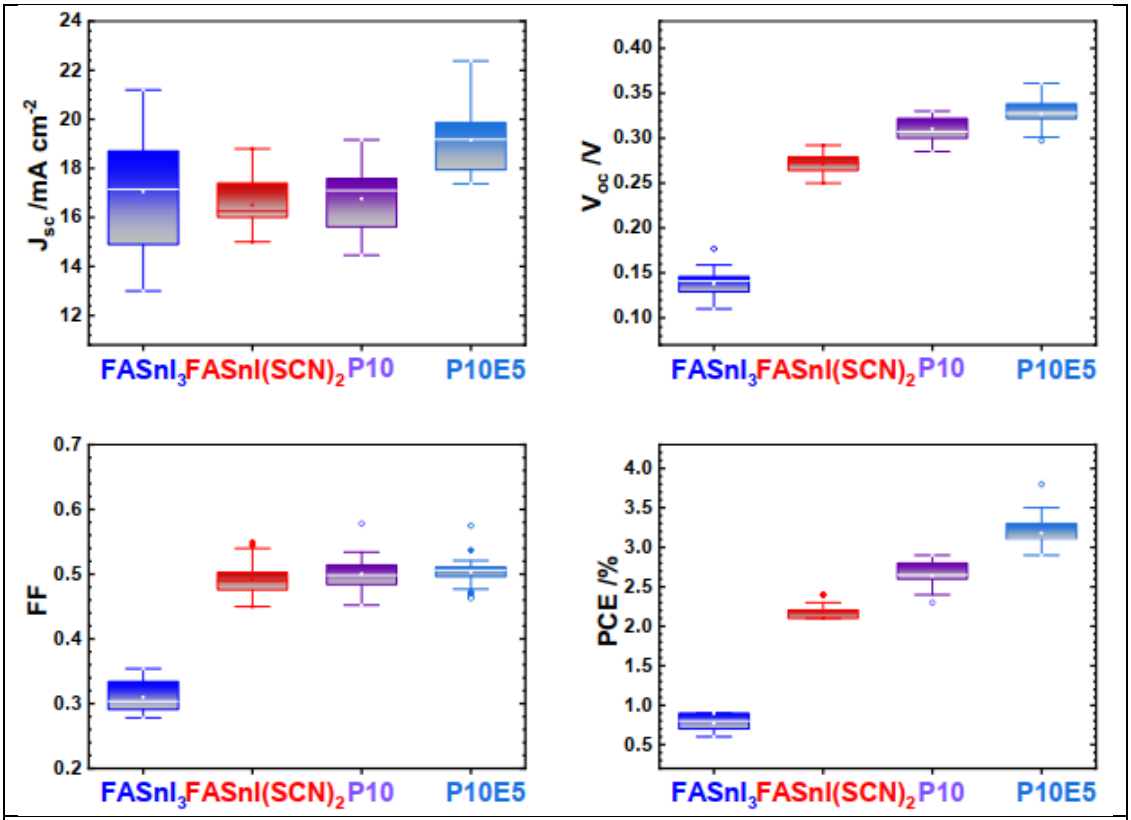


Figure 3 . Statistical distribution of 30 devices for each type of perovskite solar cell: FASnI3, FASnI(SCN)2, P10, and P10E5.[136]

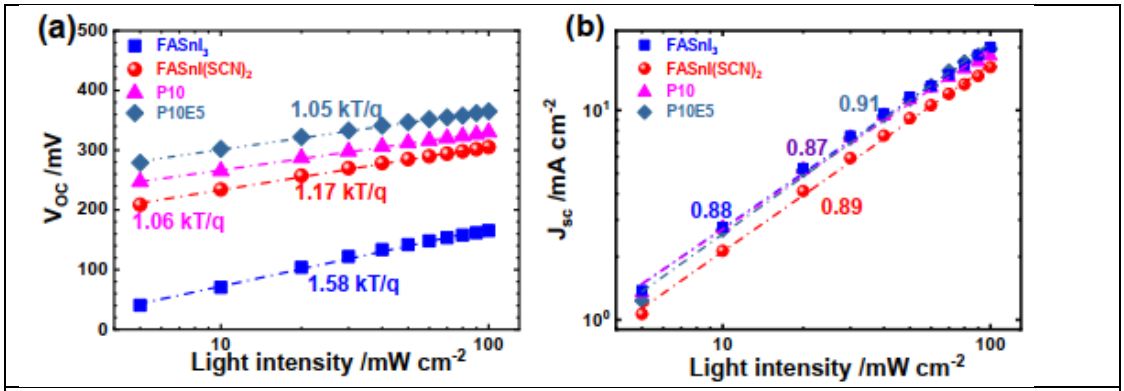


Figure 4.a,b. Dependence on light intensity of (a) open-circuit voltage (Voc) and (b) short-circuit current density (Jsc) for FASnI3, FASnI(SCN)2, P10 and P10E5 devices.[136].

4.2.1. Back-Contact and Interface Physics

The studys examined an HTL-free lead-free perovskite architecture based on FASnI3/C60, with the rear contact treated as a key optoelectronic element rather than a passive current collector. Using SCAPS-1D, the authors showed that removing the HTL simplified the device and improved performance from 12.53% to 14.46%, mainly by reducing interfacial losses and improving carrier extraction. The work also demonstrated that the rear interface is highly sensitive to defect density and energy-level alignment. Bulk defect densities above about 10^{15} cm^{-3} caused a sharp drop in Voc, Jsc, and FF, while interface defect densities in the range of 10^{14}-10^{18} cm^{-2} strongly degraded efficiency through enhanced SRH recombination and contact resistance. A similar trend was found for the back-contact work function: increasing it from 4.2 eV to around 5.0 eV improved band alignment, reduced the extraction barrier, and raised the simulated efficiency to 19.63%, with Voc = 0.87 V, Jsc = 27.86 mA/cm^2, and FF = 81%. As shown in Figure (5), The study therefore supports a clear design rule for rear-interface engineering in lead-free tin perovskites: performance is governed not only by absorber quality, but also by contact energetics, interface cleanliness, and the electrostatic profile near the

(This work is licensed under a Creative Commons Attribution 4.0 International License.)

International Journal of Engineering Research & Technology (IJERT)
ISSN: 2278-0181
Vol. 15 Issue 11 , November - 2026

back electrode. At the same time, the reported values should be read as theoretical limits from SCAPS-1D, not as direct experimental benchmarks. [138].

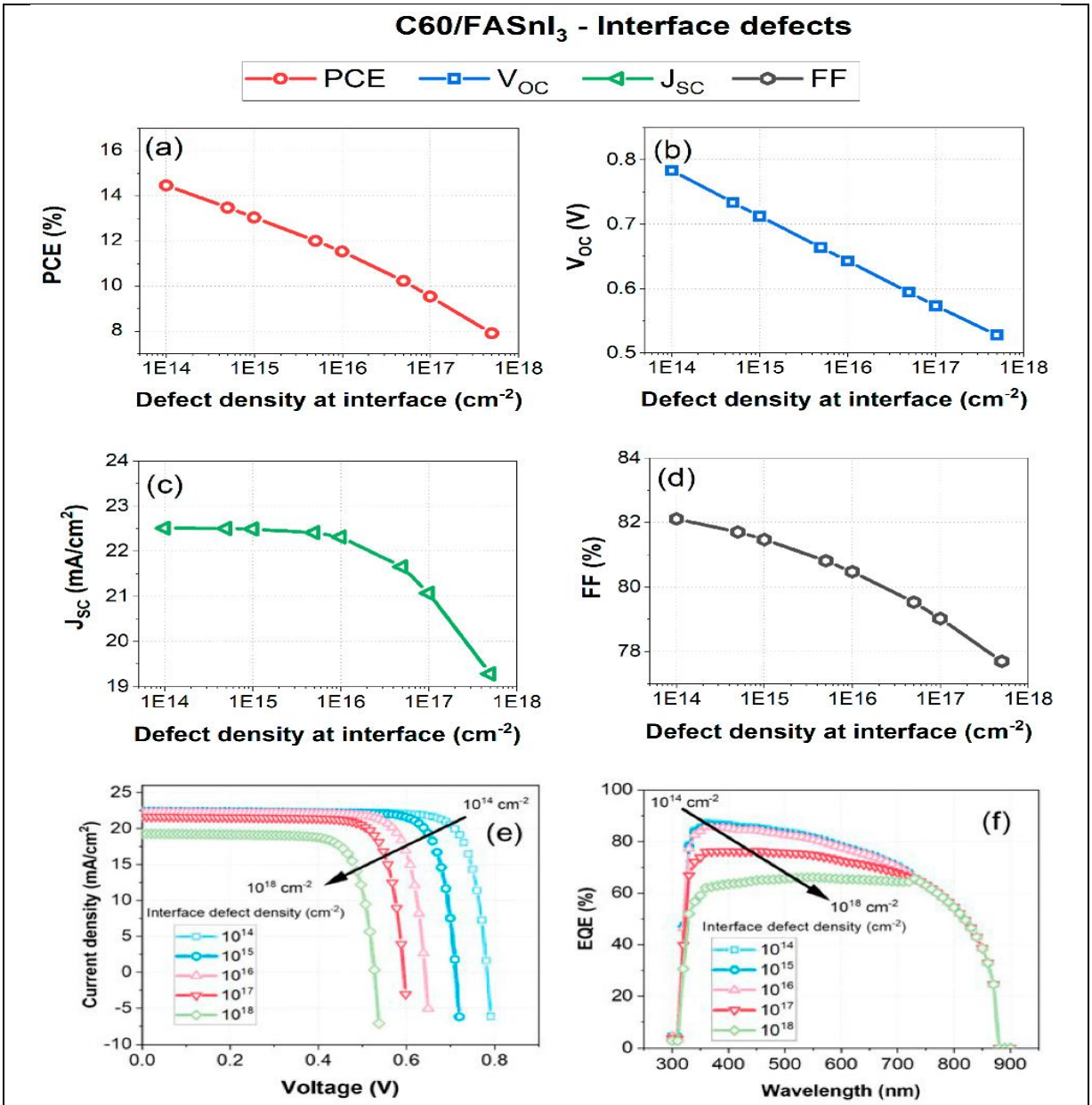
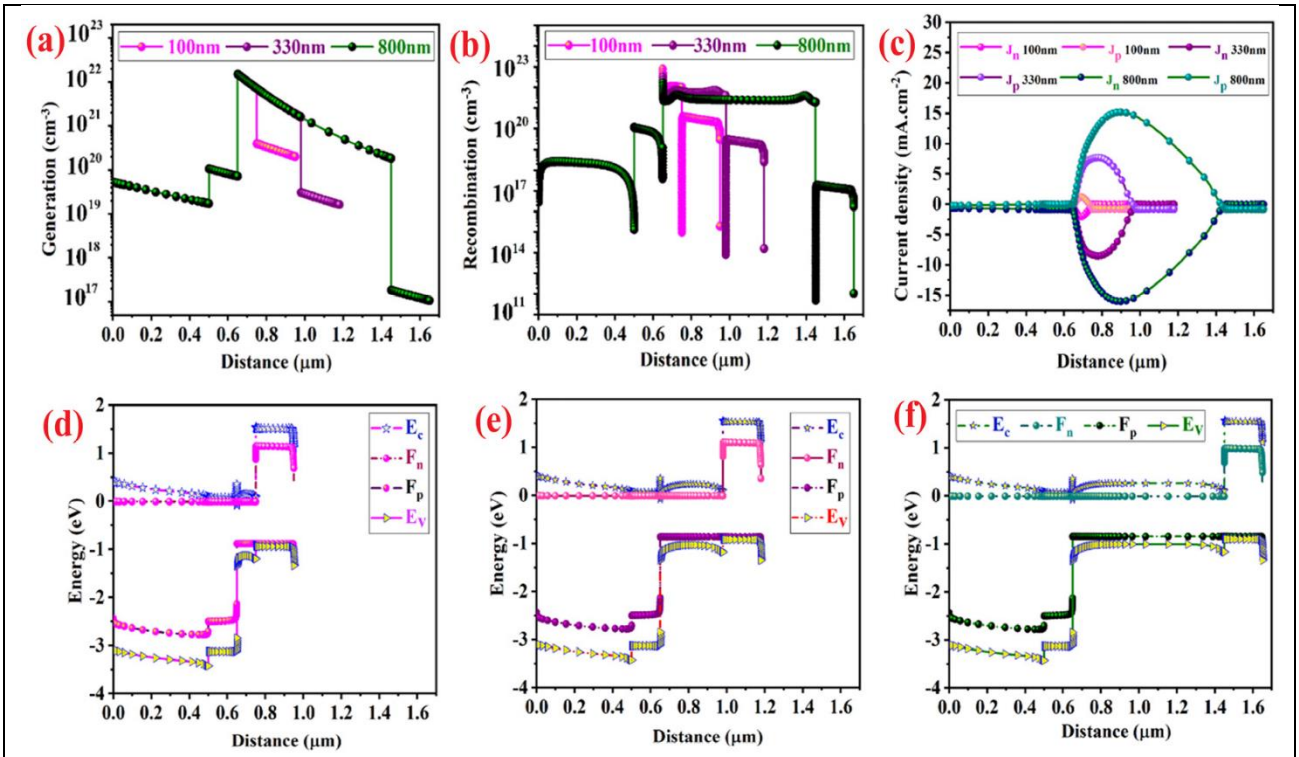


Figure (5). Impact of interface defect density on the PV performance parameters of the HTL-free FASnI3 structure: (a) PCE, (b) VOC, (c) JSC, (d) FF, (e) J-V characteristics, (f) EQE versus wavelength[138].

Seyed-Talebi et al(2023),[137]. conducted a systematic SCAPS-1D study of normal-structure $CsSnI_3$ solar cells with the architecture FTO/TiO_2/$CsSnI_3$/HTL/back contact. The work evaluated the combined effects of absorber thickness, hole-transport layer (HTL), and rear-electrode material across 120 device configurations. Initially, the simulated device containing Spiro-OMeTAD showed good agreement with a previously reported experimental efficiency of approximately 12.96% at an absorber thickness of 330 nm. Increasing the $CsSnI_3$ thickness to around 800 nm increased the calculated efficiency to approximately 18.1%,As shown in the figure (6), mainly because of enhanced light absorption and carrier generation. However, further thickening of the absorber produced limited improvement because of increased carrier-transport paths and recombination losses.[139]

(This work is licensed under a Creative Commons Attribution 4.0 International License.)

International Journal of Engineering Research & Technology (IJERT)
ISSN: 2278-0181
Vol. 15 Issue 11 , November - 2026



Figure(6) The effect of perovskite thickness modification on (a) generation rate, (b) recombination rate of photo-generated carriers per volume unit in different layers of simulated devices with different perovskite absorber thickness, (c) current density of electrons (Jn) and holes (Jp), and conduction band position (Ec), valence band position (Ev), Fermi energy levels for device with perovskite thickness of (d) 100 nm, (e) 330 nm, and (f) 800 nm.[139]

The main relevance of this study to rear-interface engineering is its comparison of ten back contacts—Ag, Cu, Fe, carbon, Au, W, Ni, Pd, Pt, and Se—in combination with different HTLs. The simulations showed that the back electrode significantly affected the fill factor, which the authors associated with changes in interfacial recombination and chain resistance at the metal/HTL junction. In several configurations, Se-, Pt-, and Pd-based contacts produce higher efficiencies than the commonly used Au electrode. However, the study did not experimentally compare these metals, and the reported trends mainly reflect the assumed work functions and interface parameters in SCAPS-1D. Therefore, the results should be interpreted as a theoretical screening of contact energetics rather than definitive evidence of the practical superiority of one metal. The study further showed that the HTL cannot be optimized independently from the rear electrode. $Cu_2ZnSnSe_4$ (CZTSe) provided the highest simulated efficiency among the investigated HTLs, reaching 21.63%, which was attributed to favorable band alignment and efficient hole transport. Overall, the work demonstrates that rear-contact performance in $CsSnI_3$ devices is governed by the coupled effects of HTL selection, value-band alignment, contact resistance, and interfacial recombination[140]. It also highlights that a suitable back contact must be evaluated as part of the complete absorber/HTL/electrode interface rather than as an isolated metal layer.[139]. An study employed an integrated multi-scale modeling framework—combining first-principles Density Functional Theory (DFT/CASTEP) with device simulation via SCAPS-1D to systematically evaluate lead-free, planar n-i-p solar cells based on $CsSnI_3$. Through a combinatorial screening process involving over 70 structural configurations—comprising seven electron transport layers (ETLs), ten hole transport layers (HTLs), and a gold (Au) back electrode—the study demonstrated that back-interface physics and energy band alignment critically determine charge carrier dynamics. Among the evaluated combinations, the ITO/PCBM/$CsSnI_3$/CuI/Au configuration achieved the best simulated photovoltaic performance, recording an open-circuit voltage (Voc) of 0.909 V, a short-circuit current density (Jsc) of 14.24 mA/cm², a fill factor (FF) of 78.11%, and a power conversion efficiency (PCE) of 10.10%. As shown in Figure (7).[140].

(This work is licensed under a Creative Commons Attribution 4.0 International License.)

International Journal of Engineering Research & Technology (IJERT)
ISSN: 2278-0181
Vol. 15 Issue 11 , November - 2026

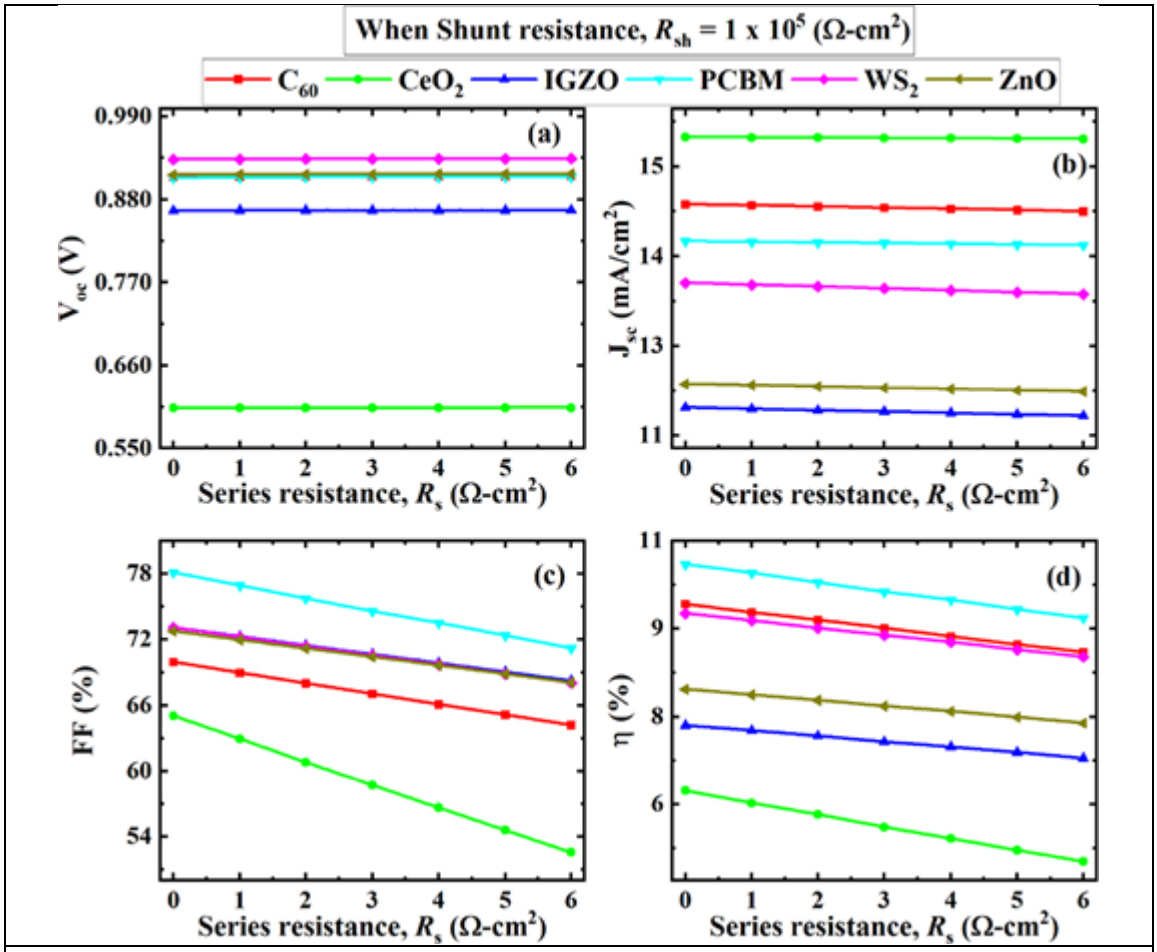


Figure (7). Effect of varying Rs on PV parameters (a) Voc, (b) Jsc, (c) FF, and (d) PCE with constant Rsh for different ETLs.[140].

The key contribution of this work to the field of back-contact physics lies in elucidating the interplay between energy level alignment and the charge carrier extraction process at the back junction. Analysis revealed that the activation energy for the interfacial recombination process is governed by the equation (Ea = Eg - |CBO/VBO|); this indicates that significant valence band offsets (VBO) at the junction between the absorber layer and the hole transport layer (HTL) substantially lower the effective energy barrier height and increase non-radiative recombination losses. Incorporating inorganic CuI as a p-type contact layer achieved optimal energy band alignment and a favorable built-in potential (Vbi)—determined via Mott–Schottky capacitance analysis—thereby mitigating charge accumulation and enhancing hole extraction toward the gold (Au) back electrode. Critically, the efficiency predicted by the modeling significantly exceeds previously recorded experimental benchmarks for pristine CsSnI3 devices (approximately 3.8%); this largely reflects idealized numerical assumptions, such as low interfacial defect density (1.0×10^{10} cm^{-2}) and the neglect of oxidation and self-doping dynamics associated with tin ions (Sn^{2+}/Sn^{4+}). Furthermore, the results highlight a common interfacial trade-off: while alternative transport materials (such as CeO2) yielded slightly higher photocurrents (Jsc ≈ 15.86 mA/cm²), they suffered a sharp drop in open-circuit voltage (Voc = 0.603 V) due to interfacial charge-carrier traps and energy level misalignment. In conclusion, this study demonstrates that improving the back contact in tin-based (lead-free) perovskite cells cannot rely solely on the conductivity of the back electrode; rather, it requires precise energy band alignment at the interface, the minimization of interfacial recombination rates, and the matching of work functions across the entire junction—comprising the CsSnI3, the hole transport layer (HTL), and the back electrode[140].

4.3. Metallic Back Contacts and Low-Work-Function Electrodes

4.3.1 Influence of Metal Work Function on Rear Contact Properties in $CsSnI_3$-Based Devices

The energy alignment at the rear interface is an important factor that affects charge collection in lead-free perovskite solar cells (LF-PSCs). **In a 2024 study**, **Park, Son[141]**, and Jeong investigated the effect of the rear metal contact in an n–i–p solar cell with the structure FTO/ZnO/$CsSnI_3$/NiO_x/Metal. Several metals with different work functions were considered, including Al (4.20 eV), Cu (4.60 eV), Ag (4.70 eV), Fe (4.80 eV), and Au (5.10 eV), as well as metals with higher work functions such as W, Ni, Pt, and Se. The numerical

(This work is licensed under a Creative Commons Attribution 4.0 International License.)

International Journal of Engineering Research & Technology (IJERT)
ISSN: 2278-0181
Vol. 15 Issue 11 , November - 2026

simulations showed that using metals with low work functions leads to the formation of a significant Schottky barrier at the NiO_x/Metal interface. This barrier makes it more difficult for holes to move from the NiO_x layer to the metal electrode. As a result, charge carriers accumulate near the interface, increasing the series resistance of the device. This causes a noticeable reduction in the fill factor (FF) and, consequently, in the overall power conversion efficiency. For example, the device using Al as the rear contact achieved a relatively low efficiency of about 4.17%. as shown in figure (8). As the metal work function increased, hole extraction became easier and the rear interface became more favorable from an energetic point of view. This improvement was particularly clear when Au, with a work function of 5.10 eV, was used. In this case, the contact showed nearly Ohmic behavior, which improved charge transport and reduced non-radiative losses at the rear interface. After optimizing the other device parameters, the Au-contacted cell achieved a simulated efficiency of 23.84%, with an open-circuit voltage (Voc) of 1.05 V, a short-circuit current density (Jsc) of 28.02 $mA \cdot cm^{-2}$, and a fill factor (FF) of 81.22%.[140].

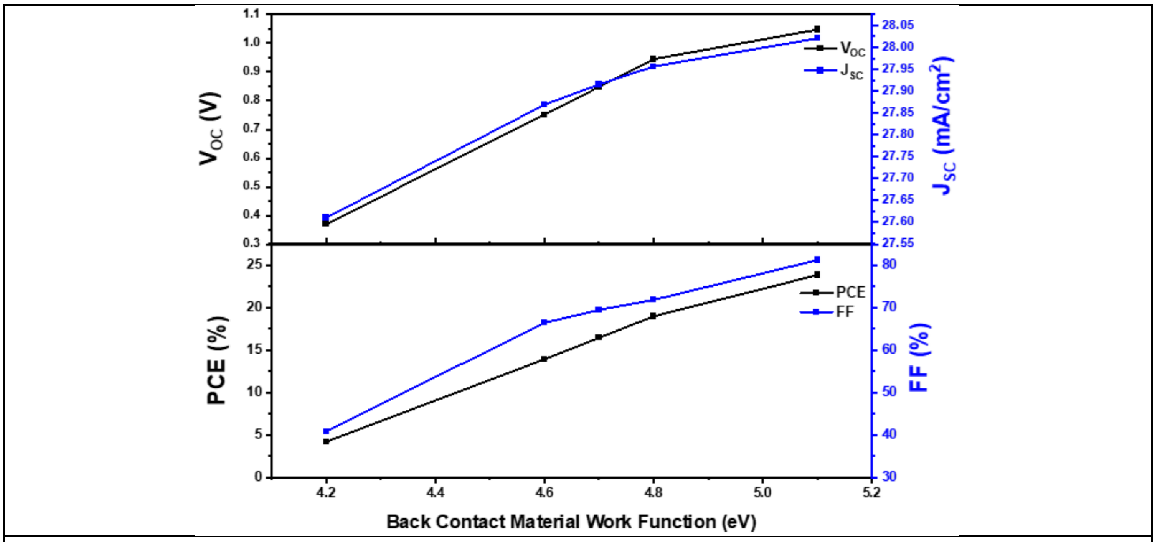


Figure (8): The variation in VOC, JSC, FF, and PCE with back contact material work function.[141].

Another important result was that increasing the metal work function beyond approximately 5.10 eV did not provide a significant further improvement in device performance. When metals such as Ni, with a work function of 5.5 eV, or Pt, with a work function of 5.7 eV, were used, the performance parameters became almost constant. This suggests that there is a certain limit beyond which the rear interface reaches a nearly Ohmic or flat-band condition. Therefore, further increasing the metal work function has little effect on charge extraction.

Overall, these results show that using a metal with a high work function can help reduce Schottky-barrier-related extraction losses in tin-based perovskite solar cells. However, it is important to note that the study was based on numerical simulations that assumed nearly ideal interfaces, with a very low interface defect density ($N_it \approx 10^8$ cm^{-2}) and without considering chemical reactions between the different materials. Therefore, the reported results mainly describe the ideal electronic and electrostatic behavior of the device. In practical devices, high-work-function metals such as Au and Pt may also introduce several challenges, including high material and fabrication costs, possible corrosion caused by halides, and metal diffusion through thin hole-transport layers. Therefore, these simulation results can mainly be considered as a useful reference for identifying the work function required to achieve a suitable rear contact. They also highlight the need to develop lower-cost, more abundant, and chemically stable alternatives that can provide similar electronic properties[141].

Danladi et al. (2023)[142], systematically investigated the effect of metallic back contacts on the performance of perovskite solar cells, considering both HTM-free and HTM-based configurations using SCAPS-1D simulations. The study examined Ag, Cr, Cu, Au, Ni, and Pt as back electrodes, with work functions of 4.47, 4.50, 4.65, 5.10, 5.15, and 5.65 eV, respectively. For the HTM-free devices, the use of low-work-function metals resulted in a clear reduction in photovoltaic performance. With Ag, the power conversion efficiency (PCE) was only 3.108%, with an open-circuit voltage (V_oc) of 0.382 V and a fill factor (FF) of 33.201%. When Cu was used, the PCE increased to 6.338%, while V_oc and FF increased to 0.562 V and 44.501%, respectively. Although the short-circuit current density (J_sc) remained relatively high, the overall efficiency was still low. This suggests that the main limitation was not the generation of

(This work is licensed under a Creative Commons Attribution 4.0 International License.)

International Journal of Engineering Research & Technology (IJERT)
ISSN: 2278-0181
Vol. 15 Issue 11 , November - 2026

charge carriers in the absorber layer, but rather their inefficient extraction through the rear contact. As the metal work function increased, both the open-circuit voltage and fill factor improved significantly, leading to a substantial increase in the overall efficiency. Devices using Au and Ni as back contacts achieved PCEs of 16.166% and 17.311%, respectively. Pt, which had the highest work function among the investigated metals, provided the best performance, with a V_oc of 1.247 V, a J_sc of 25.781 mA·cm^{-2}, and an FF of 81.596%. The resulting PCE reached 26.229%. In the HTM-based devices, the effect of the metal type on V_oc and J_sc became less pronounced. As shown in figures (9, 10)

This can be explained by the presence of the HTM layer, which acts as an intermediate layer between the absorber and the metal electrode and therefore reduces the direct influence of the metal on the absorber/metal interface. Nevertheless, the choice of the back electrode continued to have a significant effect on the fill factor and overall device efficiency. Pt again provided the highest performance, with a PCE of 25.608%, compared with 23.941% for Ni and 22.768% for Au.[142]

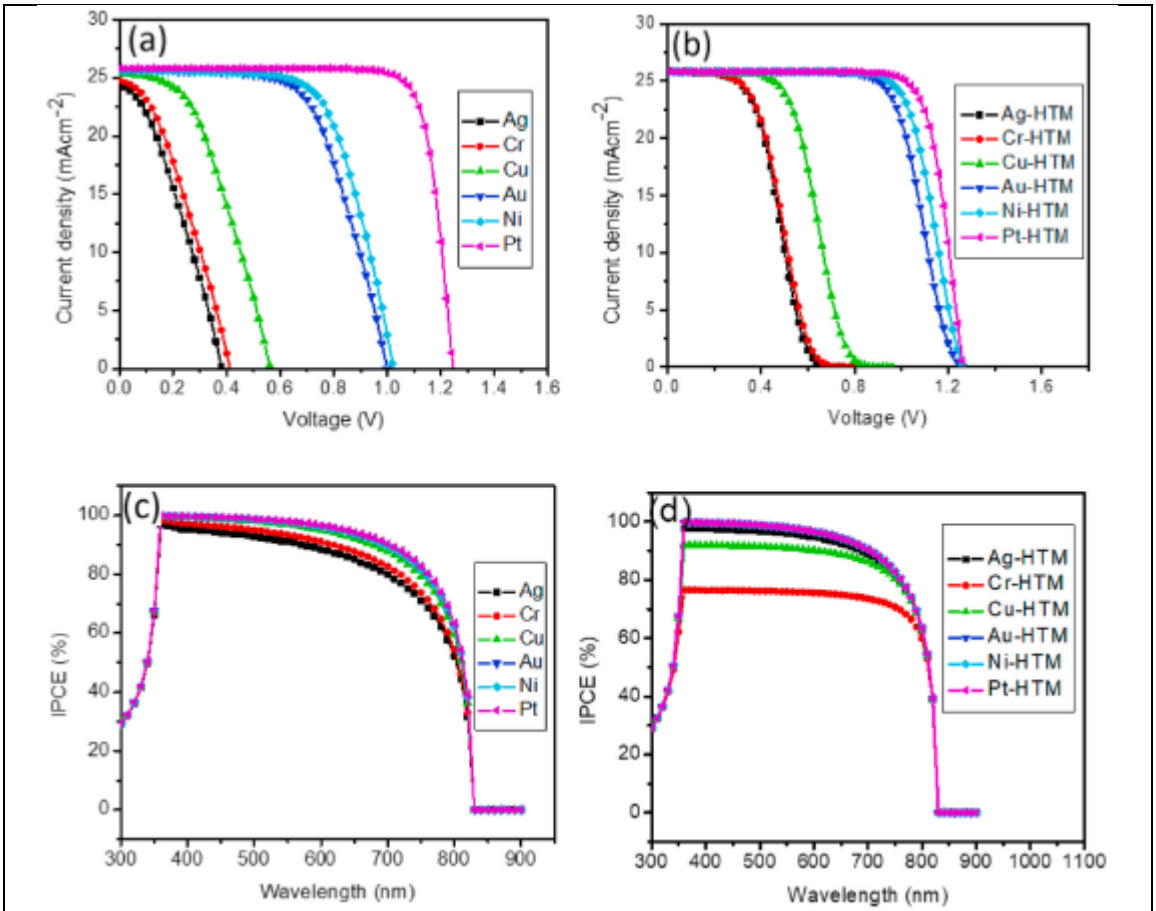


Fig. 9. (a) J-V curve with different metal contact under illumination without HTM, (b) J-V curve with different metal contact under illumination with HTM, (c) QE with respect to wavelength for HTM-free PSC and (d) QE with respect to wavelength for HTM-based PSC,[142].

(This work is licensed under a Creative Commons Attribution 4.0 International License.)

International Journal of Engineering Research & Technology (IJERT)
ISSN: 2278-0181
Vol. 15 Issue 11 , November - 2026

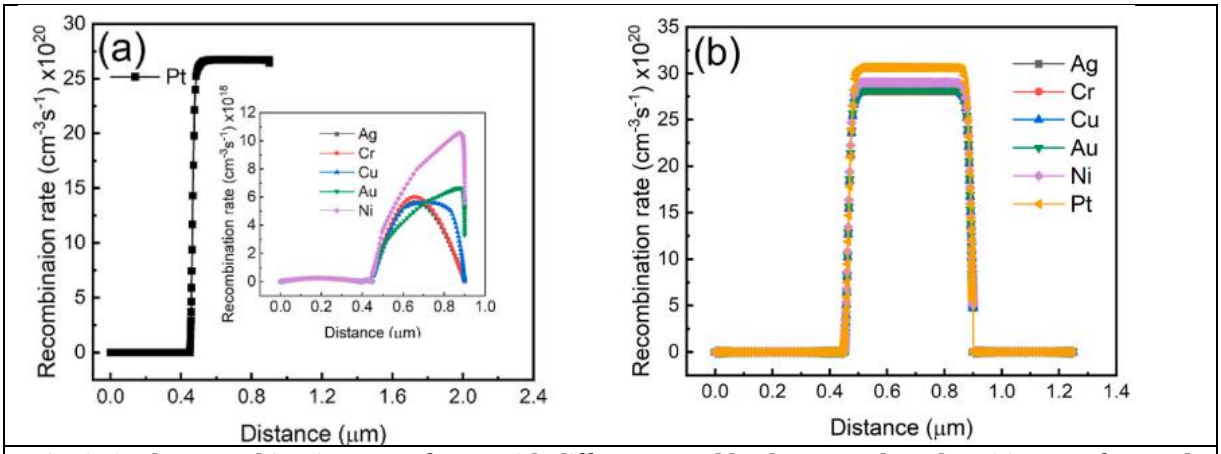


Fig. (10):The recombination rate of PSC with different metal back contact based on (a) HTM-free and (b) HTM-based device.[142].

These results show that matching the metal work function with the energy levels of the device is particularly important when the absorber is in direct contact with the rear electrode. When an HTM layer is present, the direct effect of the metal is reduced, and the properties of the HTM/metal interface and its associated contact resistance become more important in determining the overall device performance[142].

However, the predicted superiority of Pt should be interpreted with caution because the results were obtained solely from SCAPS-1D simulations. In practical applications, the use of Pt may be limited by its high cost. In addition, the study did not experimentally investigate interfacial chemical reactions, metal diffusion into the adjacent layers, or long-term device stability. Therefore, these results provide useful insight into the relationship between the work function of the back electrode and device performance, but they do not necessarily mean that Pt is the most suitable choice for practical device fabrication

4.3.2. Supporting a Multiscale Interpretation of Metal Contact Loss

Yahyaoui (2026)[143], presents a multiscale framework integrating density functional theory, device simulations using SCAPS-1D software, Lambert function-based analytical modeling, and machine learning to interpret charge transport loss and electrical loss in quantum dot and perovskite solar cells. As shown in Figure (11) Although this work does not provide an original quantitative comparison of metal back contacts in a specific lead-free perovskite structure, it does offer a useful methodological basis for analyzing contact loss. The review defines the back electrode as the final component of hole assembly in the general TCO/ETL/absorber/HTL/metal structure and discusses commonly used metal contacts, including gold, silver, aluminum, and molybdenum. Within this framework, the energy compatibility between the metal's occupation function and the valence band level of the hole transport layer or the absorber determines whether the back contact behaves as an ohmic or Schottky contact. A poorly aligned, low-work function electrode can hinder hole extraction, leading to charge buildup at the interface, increased contact resistance contribution to the overall series resistance, and reduced fill factor and power conversion efficiency. This is a significant contribution.

(This work is licensed under a Creative Commons Attribution 4.0 International License.)

International Journal of Engineering Research & Technology (IJERT)
ISSN: 2278-0181
Vol. 15 Issue 11 , November - 2026

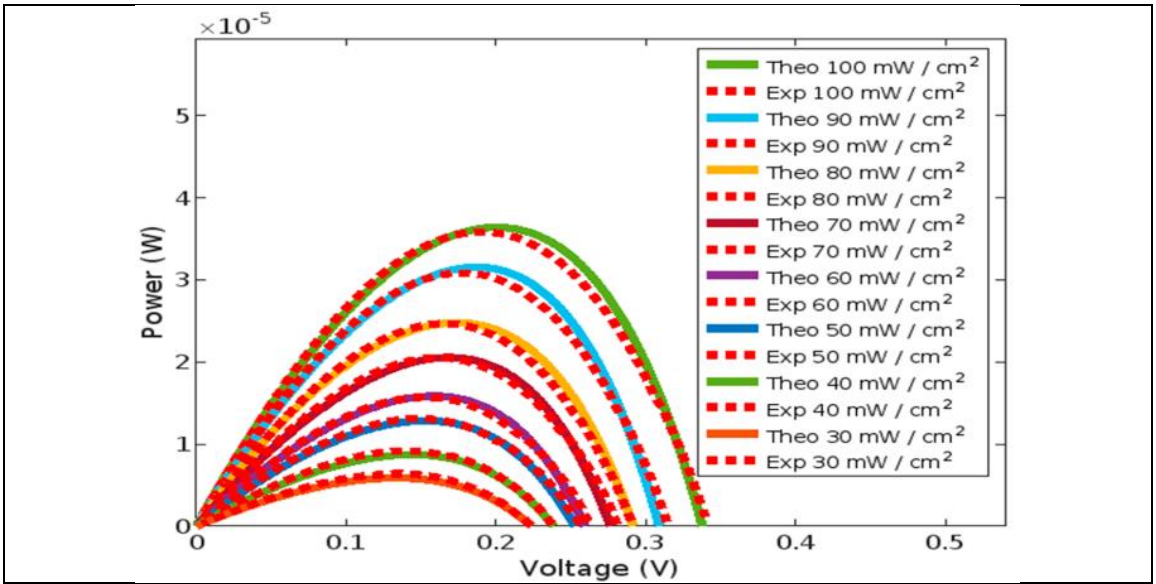


Figure (11) :Comparison of experimental and Lambert W-Modeled J−V and P−V curves.[143].

Extracting non-ideal diode parameters from J-V current-voltage (J-V) curves using the work function (W) is also a significant contribution. By isolating the effects of series resistance, parallel resistance, diode ideality factor, and reverse saturation current, this approach can help distinguish between contact resistance losses and recombination and leakage paths in the block. This distinction is crucial when evaluating back electrodes with low work functions, as the resulting performance degradation may manifest primarily as a decrease in the square of the J-V curve and a decrease in the fill factor, rather than a significant decrease in photogenerated current. The review also emphasizes that energy suitability alone is insufficient for electrode selection: corrosion, metal ion migration, and chemical reactions at the interface can generate deep recombination centers, negatively impacting long-term stability. Therefore, metallic back-conductors should be evaluated within a comprehensive framework that includes work function matching, contact resistivity extraction, interface chemistry, and operational stability. However, because this article is a systematic review and not an original comparison between metals and electrodes, its findings should be used to support a physical explanation of contact loss rather than to quantitatively classify specific metals.[143].

REFERENCES

[1] REN21, *Renewables 2023 Global Status Report*, REN21 Secretariat, Paris, 2023.
[2] International Energy Agency (IEA), *World Energy Outlook 2023*, IEA, Paris, 2023.
[3] IPCC, *Climate Change 2023: Synthesis Report*, Intergovernmental Panel on Climate Change, Geneva, 2023.
[4] M.A. Green, E.D. Dunlop, J. Hohl-Ebinger, M. Yoshita, N. Kopidakis, X. Hao, Solar cell efficiency tables (version 64), *Prog. Photovolt. Res. Appl.* 32 (2024) 3–13.
[5] A. Richter, M. Hermle, S.W. Glunz, Reassessment of the limiting efficiency for crystalline silicon solar cells, *IEEE J. Photovolt.* 3 (2013) 1184–1191.
[6] M.A. Green, Third generation photovoltaics: solar cells for 2020 and beyond, *Physica E* 14 (2002) 65–70.
[7] A. Kojima, K. Teshima, Y. Shirai, T. Miyasaka, Organometal halide perovskites as visible-light sensitizers for photovoltaic cells, *J. Am. Chem. Soc.* 131 (2009) 6050–6051.
[8] M.M. Lee, J. Teuscher, T. Miyasaka, T.N. Murakami, H.J. Snaith, Efficient hybrid solar cells based on meso-superstructured organometal halide perovskites, *Science* 338 (2012) 643–647.
[9] National Renewable Energy Laboratory (NREL), *Best Research-Cell Efficiency Chart*, Golden, CO, updated 2024.
[10] M.A. Green, A. Ho-Baillie, H.J. Snaith, The emergence of perovskite solar cells, *Nat. Photonics* 8 (2014) 506–514.
[11] F.P.G. de Arquer, A. Armin, P. Meredith, E.H. Sargent, Solution-processed semiconductors for next-generation photodetectors and solar cells, *Nat. Rev. Mater.* 2 (2017) 16100.
[12] H. Min, D.Y. Lee, J. Kim, et al., Perovskite solar cells with atomically coherent interlayers on SnO2_22 electrodes, *Nature* 598 (2021) 444–450
[13] M. Saliba, T. Matsui, J.Y. Seo, et al., Cesium-containing triple cation perovskite solar cells: improved stability, reproducibility and high efficiency, *Energy Environ. Sci.* 9 (2016) 1989–1997.
[14] H. Tsai, W. Nie, J.C. Blancon, et al., High-efficiency two-dimensional Ruddlesden–Popper perovskite solar cells, *Nature* 536 (2016) 312–316.
[15] S.D. Stranks, H.J. Snaith, Metal-halide perovskites for photovoltaic and light-emitting devices, *Nat. Nanotechnol.* 10 (2015) 391–402.
[16] G. Grancini, M.K. Nazeeruddin, Dimensional tailoring of hybrid perovskites for photovoltaics, *Nat. Rev. Mater.* 4 (2019) 4–22
[17] D.B. Mitzi, K. Chondroudis, C.R. Kagan, Design, structure, and optical properties of organic–inorganic perovskites containing tin and lead halides, *Inorg. Chem.* 38 (1999) 6246–6256.

(This work is licensed under a Creative Commons Attribution 4.0 International License.)

International Journal of Engineering Research & Technology (IJERT)
ISSN: 2278-0181
Vol. 15 Issue 11 , November - 2026

[18] G.E. Eperon, S.D. Stranks, C. Menelaou, et al., Formamidinium lead trihalide: a broadly tunable perovskite for efficient planar heterojunction solar cells, *Energy Environ. Sci.* 7 (2014) 982–988.
[19] W.-J. Yin, T. Shi, Y. Yan, Unusual defect physics in CH3_33NH3_33PbI3_33 perovskite solar cell absorber, *Appl. Phys. Lett.* 104 (2014) 063903.
[20] A.M. Ganose, C.N. Savory, D.O. Scanlon, Beyond methylammonium lead iodide: prospects for the emergent field of ns2^22-containing solar absorbers, *Chem. Commun.* 53 (2017) 20–44.
[21] M.G. Kanatzidis, Halide perovskites: poor man's high-performance semiconductors, *Nat. Mater.* 16 (2017) 899–900.
[22] J.-P. Correa-Baena, M. Saliba, T. Buonassisi, et al., Promises and challenges of perovskite solar cells, *Science* 358 (2017) 739–744.
[23] W.S. Yang, B.-W. Park, E.H. Jung, et al., Iodide management in formamidinium-lead-halide–based perovskite layers for efficient solar cells, *Science* 356 (2017) 1376–1379.
[24] T. Leijtens, G.E. Eperon, N.K. Noel, S.N. Habisreutinger, A. Petrozza, H.J. Snaith, Stability of metal halide perovskite solar cells, *Adv. Energy Mater.* 5 (2015) 1500963.
[25] J.A. Christians, P.A. Miranda Herrera, P.V. Kamat, Transformation of the excited state and photovoltaic efficiency of CH3_33NH3_33 PbI3_33 perovskite upon controlled exposure to humidified air, *J. Am. Chem. Soc.* 137 (2015) 1530–1538.
[26] N.-G. Park, Perovskite solar cells: an emerging photovoltaic technology, *Mater. Today* 18 (2015) 65–72.
[27] Y. Rong, L. Liu, A. Mei, X. Li, H. Han, Beyond efficiency: the challenge of stability in mesoscopic perovskite solar cells, *Adv. Energy Mater.* 5 (2015) 1501066.
[28] B. Zhao, S. Bai, V. Kim, et al., High-efficiency perovskite–polymer bulk heterostructure light-emitting diodes, *Nat. Photonics* 12 (2018) 783–789.
[29] R.E. Brandt, V. Stevanović, D.S. Ginley, T. Buonassisi, Identifying defect-tolerant semiconductors with high minority-carrier lifetimes: beyond hybrid lead halide perovskites, *MRS Commun.* 5 (2015) 265–275.
[30] T.M. Koh, T. Krishnamoorthy, N. Yantara, et al., Formamidinium tin-based perovskite with low Eg for photovoltaic applications, *J. Mater. Chem. A* 3 (2015) 14996–15000.
[31] T. Krishnamoorthy, H. Ding, C. Yan, et al., Lead-free germanium iodide perovskite materials for photovoltaic applications, *J. Mater. Chem. A* 3 (2015) 23829–23832.
[32] F. Hao, C.C. Stoumpos, D.H. Cao, R.P.H. Chang, M.G. Kanatzidis, Lead-free solid-state organic–inorganic halide perovskite solar cells, *Nat. Photonics* 8 (2014) 489–494.
[33] F. Hao, C.C. Stoumpos, R.P.H. Chang, M.G. Kanatzidis, Anomalous band gap behavior in mixed Sn and Pb perovskites enables broadening of absorption spectrum in solar cells, *J. Am. Chem. Soc.* 136 (2014) 8094–8099.
[34] W. Ke, C.C. Stoumpos, M.G. Kanatzidis, "Unleaded" perovskites: status quo and future prospects of tin-based perovskite solar cells, *Adv. Mater.* 31 (2019) 1803230.
[35] T. Bin Song, T. Yokoyama, S. Aramaki, M.G. Kanatzidis, Performance enhancement of lead-free tin-based perovskite solar cells with reducing atmosphere-assisted dispersible additive, *ACS Energy Lett.* 2 (2017) 897–903.
[36] A. Abate, Perovskite solar cells go lead free, *Joule* 1 (2017) 659–664.
[37] W. Ke, M.G. Kanatzidis, Prospects for low-toxicity lead-free perovskite solar cells, *Nat. Commun.* 10 (2019) 965.
[38] C.C. Stoumpos, C.D. Malliakas, M.G. Kanatzidis, Semiconducting tin and lead iodide perovskites with organic cations: phase transitions, high mobilities, and near-infrared photoluminescent properties, *Inorg. Chem.* 52 (2013) 9019–9038.
[39] Y. Shao, Y. Yuan, J. Huang, Correlation of energy disorder and open-circuit voltage in hybrid perovskite solar cells, *Nat. Energy* 1 (2016) 15001.
[40] N.K. Noel, S.D. Stranks, A. Abate, et al., Lead-free organic–inorganic tin halide perovskites for photovoltaic applications, *Energy Environ. Sci.* 7 (2014) 3061–3068.
[41] I. Chung, B. Lee, J. He, R.P.H. Chang, M.G. Kanatzidis, All-solid-state dye-sensitized solar cells with high efficiency using perovskite absorbers, *Nature* 485 (2012) 486–489.
[42] A. Marshall, R.E. Brandt, D.H. Cao, et al., Cesium tin halide perovskites for photovoltaics: composition and phase engineering, *J. Phys. Chem. Lett.* 11 (2020) 620–627.
[43] B. Pospischil, M.M. Tavakoli, H. Han, Stability issues in tin halide perovskites, *Adv. Funct. Mater.* 31 (2021) 2008185
[44] J. Heo, J.H. Im, Y. Heo, K. Lee, T.K. Ahn, N.-G. Park, Efficient inorganic–organic hybrid heterojunction solar cells containing perovskite compound and polymeric hole conductors, *Nat. Photonics* 7 (2013) 486–491
[45] H.J. Park, SCAPS-1D simulation for device optimization to improve efficiency in lead-free CsSnI3_33 perovskite solar cells, *Inorganics* 12 (2024) 123.
[46] E. Danladi, S.A. Alatawi, A.A. Alharthi, et al., 20.730% highly efficient lead-free CsSnI3_33-based perovskite solar cells with various charge transport materials: a SCAPS-1D study, *Multiscale Multidiscip. Model. Exp. Des.* 8 (2024) 114
[47] A Comprehensive Study of CsSnI3_33-Based Perovskite Solar Cells with Efficient Charge Transport Materials and Various Metal Back Contacts, *Micromachines* 14 (2023) 1562.
[48] T.M. Koh, T. Krishnamoorthy, N. Yantara, et al., Formamidinium tin-based perovskite with low Eg for photovoltaic applications, *J. Mater. Chem. A* 3 (2015) 14996–15000.
[49] L. Ran, W. Ke, C.C. Stoumpos, M.G. Kanatzidis, Tin halide perovskite solar cells in the spotlight: stability and efficiency, *Adv. Energy Mater.* 10 (2020) 1903191.
[50] C. Liu, W. Li, C. Zhang, et al., Efficient lead-free FASnI3_33 perovskite solar cells enabled by interface engineering, *J. Mater. Chem. A* 8 (2020) 10337–10345
[51] Y. Wang, T. Zhang, M. Kan, Y. Zhao, Bifunctional stabilization of all-inorganic α-CsPbI3_33 perovskite for 17% efficiency photovoltaics, *J. Am. Chem. Soc.* 140 (2018) 12345–12348.
[52] A. Mei, X. Li, L. Liu, et al., A hole-conductor–free, fully printable mesoscopic perovskite solar cell with high stability, *Science* 345 (2014) 295–298.
[53] F. Di Giacomo, H. Razza, F. Matteocci, et al., High efficiency and stable perovskite solar cells with low-temperature carbon-based electrodes, *Adv. Energy Mater.* 5 (2015) 1401808.

(This work is licensed under a Creative Commons Attribution 4.0 International License.)

International Journal of Engineering Research & Technology (IJERT)
ISSN: 2278-0181
Vol. 15 Issue 11 , November - 2026

[54] X. Zhang, M. Liu, W. Eperon, et al., Carbon-based materials for perovskite solar cells, *Adv. Energy Mater.* 8 (2018) 1702498.
[55] N. Kumar, M. Chandra, M. Muddassir, Progress in MASnI3_33-based lead-free perovskite solar cells, *Sol. Energy Mater. Sol. Cells* 230 (2021) 111216.
[56] D. Sabba, H.K. Mulmudi, R.R. Prabhakar, et al., Impact of anionic Br substitution on open circuit voltage in lead free perovskite (CsSnI3_33) solar cells, *J. Phys. Chem. C* 119 (2015) 1763–1767.
[57] W. Ke, C.C. Stoumpos, J.L. Logsdon, et al., Enhancing lead-free tin halide perovskite solar cell performance through oxidation suppression, *J. Am. Chem. Soc.* 138 (2016) 14998–15003
[58] N. Noel, A. Abate, S.D. Stranks, et al., Enhanced performance in tin halide perovskite solar cells by controlled interfaces and contacts, *ACS Nano* 8 (2014) 9815–9821.
[59] M. Jørgensen, K. Norrman, F.C. Krebs, Stability/degradation of polymer solar cells, *Sol. Energy Mater. Sol. Cells* 92 (2008) 686–714.
[60] D. Sabba, H.K. Mulmudi, R.R. Prabhakar, et al., Mixed-halide tin perovskites for lead-free photovoltaics, *J. Phys. Chem. C* 119 (2015) 1763–1767.
[61] Y. Ogomi, A. Morita, S. Tsukamoto, et al., CH3_33NH3_33Snx_xxPb1−x_{1-x}1−xI3_33 perovskite solar cells covering up to 1060 nm, *J. Phys. Chem. Lett.* 5 (2014) 1004–1011.
[62] G.E. Eperon, V.M. Burlakov, P. Docampo, et al., Morphological control for high performance, solution-processed planar heterojunction perovskite solar cells, *Adv. Funct. Mater.* 24 (2014) 151–157.
[63] H.J. Park, Band alignment and bromide-content effects in mixed-halide lead-free perovskite absorbers, *J. Mater. Sci. Mater. Electron.* 35 (2024) 1–14
[64] H.J. Snaith, Present status and future prospects of perovskite photovoltaics, *Nat. Mater.* 17 (2018) 372–376.
[65] E.T. Hoke, D.J. Slotcavage, E.R. Dohner, et al., Reversible photo-induced trap formation in mixed-halide hybrid perovskites for photovoltaics, *Chem. Sci.* 6 (2015) 613–617.
[66] A.H. Slavney, T. Hu, A.M. Lindenberg, H.I. Karunadasa, A bismuth-halide double perovskite with long carrier recombination lifetime for photovoltaic applications, *J. Am. Chem. Soc.* 138 (2016) 2138–2141.
[67] E.T. McClure, M.R. Ball, W. Windl, P.M. Woodward, Cs2_22AgBiX6_66 (X = Br, Cl): new visible light absorbing, lead-free halide perovskite semiconductors, *Chem. Mater.* 28 (2016) 1348–1354.
[68] F. Giustino, H.J. Snaith, Toward lead-free perovskite solar cells, *ACS Energy Lett.* 1 (2016) 1233–1240
[69] A.H. Slavney, L. Leppert, D.O. Scanlon, H.I. Karunadasa, Defect-induced band-edge reconstruction of a bismuth-halide double perovskite for visible-light absorption, *J. Am. Chem. Soc.* 139 (2017) 5015–5018.
[70] A. Hossain, S. Kiran, M.M. Rahman, Recent progress in Cs2_22AgBiBr6_66 double perovskite solar absorbers, *Sol. RRL* 6 (2022) 2100894.
[71] M. Shrivastav, A. Pandey, P. Sharma, Improving Cs2_22AgBiBr6_66-based solar cell performance via transport-layer optimization, *Mater. Today Commun.* 36 (2023) 106761.
[72] S. Ahmad, M. Nazeeruddin, T. Brown, Contact and transport layer engineering in double perovskite photovoltaics, *J. Phys. Chem. Lett.* 11 (2020) 10114–10124.
[73] M. Toki, S. Rahman, M. Shahiduzzaman, Numerical design of inorganic charge-transport layers for Cs2_22AgBiBr6_66 solar cells, *Semicond. Sci. Technol.* 38 (2023) 015005.
[74] S. Hoefler, G. Trimmel, T. Rath, Progress on lead-free metal halide perovskites for photovoltaic applications: a review, *Monatsh. Chem.* 148 (2017) 795–826.
[75] A.M. Ganose, C.N. Savory, D.O. Scanlon, Beyond methylammonium lead iodide: prospects for the emergent field of ns2^22-containing solar absorbers, *Chem. Commun.* 53 (2017) 20–44.
[76] T. Rath, W. Peng, R. Huber, et al., Perovskite-inspired materials for photovoltaics and beyond—from design to devices, *Adv. Energy Mater.* 11 (2021) 2002922.
[77] H.J. Snaith, A. Abate, J.M. Ball, et al., Anomalous hysteresis in perovskite solar cells, *J. Phys. Chem. Lett.* 5 (2014) 1511–1515.
[78] Q. Dong, Y. Fang, Y. Shao, et al., Electron-hole diffusion lengths > 175 μm in solution-grown CH3_33NH3_33PbI3_33 single crystals, *Science* 347 (2015) 967–970.
[79] S.M. Sze, K.K. Ng, *Physics of Semiconductor Devices*, 3rd ed., Wiley, Hoboken, 2007.
[80] P. Würfel, U. Würfel, *Physics of Solar Cells: From Basic Principles to Advanced Concepts*, 3rd ed., Wiley-VCH, Weinheim, 2016.
[81] J. Bisquert, *The Physics of Solar Cells: Perovskites, Organics, and Photovoltaic Fundamentals*, CRC Press, Boca Raton, 2018.
[82] J.A. Christians, R.C.M. Fung, P.V. Kamat, An inorganic hole conductor for organo-lead halide perovskite solar cells. Improved hole conductivity with copper iodide, *J. Am. Chem. Soc.* 136 (2014) 758–764.
[83] K. Domanski, J.-P. Correa-Baena, N. Mine, et al., Not all that glitters is gold: metal-migration-induced degradation in perovskite solar cells, *ACS Nano* 10 (2016) 6306–6314.
[84] J.H. Noh, S.H. Im, J.H. Heo, T.N. Mandal, S.I. Seok, Chemical management for colorful, efficient, and stable inorganic–organic hybrid nanostructured solar cells, *Nano Lett.* 13 (2013) 1764–1769.
[85] J.A. Christians, J.S. Manser, P.V. Kamat, Best practices in perovskite solar cell efficiency measurements. Avoiding the error of making bad cells look good, *J. Phys. Chem. Lett.* 6 (2015) 852–857.
[86] M. Abdi-Jalebi, Z. Andaji-Garmaroudi, S.D. Stranks, et al., Maximizing and stabilizing luminescence from halide perovskites with potassium passivation, *Nature* 555 (2018) 497–501.
[87] H.J. Park, Work-function dependent back-contact engineering in lead-free perovskite solar cells, *Appl. Opt.* 64 (2025) 4818–4828.
[88] A. Fakharuddin, L. Schmidt-Mende, G. Garcia-Belmonte, R. Jose, I. Mora-Seró, Interfaces in perovskite solar cells, *Adv. Energy Mater.* 7 (2017) 1700623.
[89] D. Crespo-Quesada, T. Miyasaka, Carbon and graphene-derived electrodes in perovskite solar cells, *ChemSusChem* 12 (2019) 4512–4528.
[90] M. Burgelman, P. Nollet, S. Degrave, Modelling polycrystalline semiconductor solar cells, *Thin Solid Films* 361–362 (2000) 527–532.
[91] M. Burgelman, K. Decock, A. Niemegeers, J. Verschraegen, S. Degrave, SCAPS manual and application examples, University of Gent, Belgium, 2019.

(This work is licensed under a Creative Commons Attribution 4.0 International License.)

International Journal of Engineering Research & Technology (IJERT)
ISSN: 2278-0181
Vol. 15 Issue 11 , November - 2026

[92] V.H.D. Araújo, A.F. Nogueira, J.C. Tristão, L.J.D. Santos, Advances in lead-free perovskite solar cell design via SCAPS-1D simulations, *RSC Sustainability* 3 (2025) 4314–4335.
[93] Simon M. Sze, Kwok K. Ng , Physics of Semiconductor Devices, 3rd Edition, ISBN: 978-0-470-06832-8, April 2006, 832 pages, https://www.wiley.com/en-us/shop/general-introductory-electrical-electronics-engineering/physics-of-semiconductor-devices-3rd-edition-p-9780470068328.
[94] Talal H. Alzanki, Kandil M. Kandil, Adapting Integrated High Concentrated PV Modules and Evacuated Tube Collectors to Minimize Building Energy Consumption in Hot Climate, Smart Grid and Renewable Energy, Vol.10 No.10, October 23, 2019, https://www.scirp.org/reference/referencespapers?referenceid=2640362.
[95] Samia Sayed Mustafa Shaban, The Solar Cell Parameters as a Function of Its Temperature in Relation to Its Diurnal Efficiency, Optics and Photonics Journal, Vol.10 No.1, February 20, 2020, https://www.scirp.org/reference/referencespapers?referenceid=2683227.
[96] L. J. Chen, C. R. Lee, Y. J. Chuang, Z. H. Wu, and C. Chen,"Synthesis and Optical Properties of Lead-Free Cesium Tin Halide Perovskite Quantum Rods with High-Performance Solar Cell Application," Journal of Physical Chemistry Letters, vol. 7, no. 24, pp. 5028–5035, Dec. 2016, doi: 10.1021/acs.jpclett.6b02344.
[97] A. Rajagopal, K. Yao, and A. K. Y. Jen, "Toward Perovskite Solar Cell Commercialization: A Perspective and Research Roadmap Based on Interfacial Engineering," *Advanced Materials*, vol. 30, no. 32, Art. no. 1800455, 2018. https://doi.org/10.1002/adma.201800455.
[98] W. S. Yang, J. H. Noh, N. J. Jeon, Y. C. Kim, S. Ryu, J. Seo, and S. I. Seok, "Iodide Management in Formamidinium-Lead-Halide-Based Perovskite Layers for Efficient Solar Cells," *Science*, vol. 356, no. 6345, pp. 1376–1379
[99] Ossila, "Spiro-OMeTAD (Spiro-MeOTAD) | >99.0% | 207739-72-8," *Ossila Product Database*. [Online]. Available: https://www.ossila.com/products/spiro-ometad.
[100] Mohammad Sharabi, Muwaffaq Raqia, Saeed Mandou, Improving the Performance of Lead-Free Perovskite Solar Cells Using Cost-Effective Gold Substitutes via Numerical Simulation, Idlib University Journal of Research, Volume 9, Issue 1, 2026..
[101] Das, A.; Peu, S.D.; Akanda, M.A.M.; Salah, M.M.; Hossain, M.S.; Das, B.K. Numerical Simulation and Optimization of Inorganic Lead-Free Cs3Bi2I9-Based Perovskite Photovoltaic Cell: Impact of Various Design Parameters. Energies 2023, 16, 2328. https://doi.org/10.3390/en16052328.
[102] R. Tala-Ighil Zaïr, C. Oudjehani, and K. Tighilt, "SCAPS Simulation for Perovskite Solar Cell," *Journal of Solar Energy Research Updates*, vol. 8, pp. 21–26, Oct. 2025. doi: 10.31875/2410-2199.2021.08.3.
[103] O. A. Muhammed, D. Eli, P. H. Boduku, J. Tasiu, M. S. Ahmad, and N. Usman, "Modeling and simulation of lead-free perovskite solar cell using SCAPS-1D," *East European Journal of Physics*, vol. 2021, no. 2, pp. 146–154, 2021. doi: 10.26565/2312-4334-2021-2-12.
[104] K. D. Jayan and V. Sebastian, "Comprehensive device modelling and performance analysis of MASnI3 based perovskite solar cells with diverse ETM, HTM and back metal contacts," *Solar Energy*, vol. 217, pp. 40–48, Mar. 2021. doi: 10.1016/j.solener.2021.01.058.
[105] M. K. Hossain *et al.*, "Deep Insights into the Coupled Optoelectronic and Photovoltaic Analysis of Lead-Free CsSnI3 Perovskite-Based Solar Cell Using DFT Calculations and SCAPS-1D Simulations," *ACS Omega*, vol. 8, no. 25, pp. 22466–22485, Jun. 2023. doi: 10.1021/acsomega.3c00306.
[106] Seyed-Talebi SM, Mahmoudi M, Lee CH. A Comprehensive Study of $CsSnI_3$-Based Perovskite Solar Cells with Different Hole Transporting Layers and Back Contacts. Micromachines (Basel). 2023 Aug 6;14(8):1562. PMID: 37630098; PMCID: PMC10456552. doi: 10.3390/mi14081562.
[107] Shockley, W.; Read, W. T. Statistics of the recombinations of holes and electrons. Phys. Rev. 1952, 87, 835–842.
[108] Noel, N. K.; Stranks, S.D.; Abate, A.; Wehrenfennig, C.; Guarnera, S.; Haghighirad, A.-A.; Sadhanala, A.; Eperon, G.E.; Pathak, S. K.; Johnston, M.B.; Petrozza, A.; Herz, L.M.; Snaith, H. J. Lead-Free Organic–Inorganic Tin Halide Perovskites for Photovoltaic Applications. Energy Environ. Sci. 2014, 7, 3061–3068
[109] Koh, T.M.; Krishnamoorthy, T.; Yantara, N.; Shi, C.; Leong, W.L.; Boix, P.P.; Grätzel, M.; Mathews, N.; Mhaisalkar, S. G. Formamidinium Tin-Based Perovskite with Low Eg for Photovoltaic Applications. J. Mater. Chem. A 2015, 3, 14996–15000.
[110] Ke, W.; Stoumpos, C.C.; Kanatzidis, M. G. "Unleaded" Perovskites: Status Quo and Future Prospects of Tin-Based Perovskite Solar Cells. Adv. Mater. 2019, 31, 1803230
[111] Slavney, A.H.; Hu, T.; Lindenberg, A.M.; Karunadasa, H. I. A Bismuth-Halide Double Perovskite with Long Carrier Recombination Lifetime for Photovoltaic Applications. J.Am. Chem. Soc. 2016, 138, 2138–2141.
[112] Huang, Y.; Kavanagh, S. R.; Scanlon, D. O.; Walsh, A.; Hoye, R. L. Z. Perovskite-inspired materials for photovoltaics and beyond—from design to devices. Nanotechnology 2021, 32, 132004.
[113] Seyed-Talebi SM, Mahmoudi M, Lee CH. A Comprehensive Study of $CsSnI_3$-Based Perovskite Solar Cells with Different Hole Transporting Layers and Back Contacts. Micromachines (Basel). 2023 Aug 6;14(8):1562. PMID: 37630098; PMCID: PMC10456552. doi: 10.3390/mi14081562.
[114] N. Sultana, O. Islam, Z. H. Mahmood, and N. Ara Sultana, "Utilization of low cost metals as back contact with Perovskite Solar Cell," 2017. [Online]. Available: https://www.researchgate.net/publication/323735275
[115] Iglesias, M.; et al. Carbon electrodes and low-cost structures for perovskite solar cells. Electronics 2021, 10, 1145. Available at: https://www.mdpi.com/2079-9292/10/10/1145
[116] Habesrotinger, S.N.; Ligtens, T.; Eberon, J.E.; Strunks, S.D.; Nicholas, R.J.; Snaith, H.J. Carbon electrodes for high-efficiency perovskite photovoltaic cells. Nano Letters 2014, 14, 5561-5568.
[117] Chang, H.; et al. Integration of carbon electrodes and contact architecture for perovskite solar cells. Advances in Photovoltaics: Research and Applications 2024. DOI: 10.1002/pip.70053.
[118] Chen, P., et al. Stabilization of perovskite solar cells through interfacial and electrode engineering. Communications Materials 2022. Available at: https://www.nature.com/articles/s43246-022-00281-z
[119] Khan, M. A., et al. Effect of hole-transporting material on perovskite solar cells with different metallic electrodes: SCAPS-1D simulation view. Scientific Reports 2023. Available at: https://pmc.ncbi.nlm.nih.gov/articles/PMC10258428/
[120] Michaelson, H. B. Occupational Function and Periodicity of Elements. Journal of Applied Physics 1977, 48, 4729–4733.

(This work is licensed under a Creative Commons Attribution 4.0 International License.)

International Journal of Engineering Research & Technology (IJERT)
ISSN: 2278-0181
Vol. 15 Issue 11 , November - 2026

[121] Busch, K. A.; et al. Thermal and environmental stability of perovskite solar cells through contact and interface control. ACS Energy Letters 2016, 1, 428–435.
[122] Cha, J. H.; et al. Air-stable transparent heterojunction of silver iodide and copper iodide. ACS Materials and Interface Applications 2017. DOI: 10.1021/acsami.7b14378
[123] Ki, W.; Stombos, S. S.; Kanatzidis, M. J. "Lead-free perovskites": Current status and future prospects for tin-based perovskite solar cells. Advanced Materials 2019, 31, 1803230. DOI: 10.1002/adma.201803230.
[124] Slavny, A.H.; Ho, T.; Lindenburg, A.M.; Caronadasa, H.E. Long-life, charge-carrier bismuth halide perovskite for photovoltaic applications. Journal of the American Chemical Society 2016, 138, 2138-2141. DOI: 10.1021/jacs.5b13294.
[125] Maclure, E.T.; Paul, M.R.; Wendell, W.; Ertkin, E.C. AgBiX6 (X = Br, Cl): Novel lead-free, visible-light-absorbing halide perovskite semiconductor. Chemistry of Materials 2016, 28, 1348-1354.
[126] Huang, Y.-T.; Kavanagh, S.R.; Scanlon, D.O.; Walsh, A.; Hui, R.L.Z. Perovskite-inspired materials for photovoltaics and beyond—from design to devices. Nanotechnology 2021, 32, 132004. DOI: 10.1088/1361-6528/abcf6d.
[127] Hui, R.L.Z.; et al. Advances in lead-free, perovskite-inspired absorber materials for photovoltaics: charge transfer, defects, and device limitations. Advanced Functional Materials 2021, 2105898. DOI: 10.1002/adfm.202105898.
[128] Y. Raoui, H. Ez-Zahraouy, N. Tahiri, O. El Bounagui, S. Ahmad, and S. Kazim, "Performance analysis of MAPbI3 based perovskite solar cells employing diverse charge selective contacts: Simulation study," *Solar Energy*, vol. 193, pp. 948–955, Nov. 2019, doi: 10.1016/j.solener.2019.10.009.
[129] A. K. Kang, M. H. Zandi, and N. E. Gorji, "Simulation analysis of graphene contacted perovskite solar cells using SCAPS-1D," *Opt Quantum Electron*, vol. 51, no. 4, Apr. 2019, doi: 10.1007/s11082- 019-1802-3.
[130] S. Wang, T. Sakurai, W. Wen, and Y. Qi, "Energy Level Alignment at Interfaces in Metal Halide Perovskite Solar Cells," Nov. 23, 2018, *Wiley-VCH Verlag*. doi: 10.1002/admi.201800260.
[131] Muhammad Haneef, Sofia Tahir, Haitham A. Mahmoud, Adnan Ali, Arslan Ashfaq; Optimizing Lead-free MASnBr3 Perovskite Solar Cells for High-Efficiency and Long-Term Stability Using Graphene and Advanced Interface Layers. ACS Omega 13 February 2024; 9(6): 7053–7060. https://doi.org/10.1021/acsomega.3c08981.
[132] Sabbah, H.; Arayro, J.; Mezher, R. Numerical Simulation and Optimization of Highly Stable and Efficient Lead-Free Perovskite FA1−xCsxSnI3-Based Solar Cells Using SCAPS. Materials 2022, 15, 4761. https://doi.org/10.3390/ma15144761.
[133] Navdeep Kaur, Jaya Madan, Rahul Pandey, Maximizing photovoltaic performance of all-inorganic perovskite CsSnI3-xBrx solar cells through bandgap grading and material design, Solar Energy, Date: 15 May 2024, Article: 112573, Volume: Volume 274, 10.1016/j.solener.2024.112573.
[134] Cheng-Min Tsai,1 Yu-Pei Lin,1 Murali Krishna Pola,1 Sudhakar Narra,1 Efat Jokar,1Yaw-Wen Yang2 and Eric Wei-Guang Diau, Control of Crystal Structures and Optical Properties with Hybrid Formamidinium and 2-Hydroxyethylammonium Cations for Mesoscopic Carbon-electrode Tin-based Perovskite Solar Cells, Downloaded from pubs.acs.org/aelccp/article-supplement/682482/pdf/nz8b01046_si_001/ by guest on 24 August 2026.
[135] Mohammad Rameez,1,2,3 Saeed Shahbazi,1 Putikam Raghunath,1 Ming Chang Lin,1,4 Chen Hsiung, Hung,*,2 and Eric Wei-Guang Diau, Development of Novel Mixed Halide/Superhalide, Tin-based Perovskites for Mesoscopic Carbonbased Solar Cells. Downloaded from pubs.acs.org/jpclcd/article-supplement/502516/pdf/jz0c00479_si_001/ by guest on 24 August 2026.
[136] Mohammad Rameez,1, 2 & 3 Eric Yan-Ru Lin,1 Putikam Raghunath,1 Sudhakar Narra,1Donghoon Song,1 Ming Chang Lin,1, 4 Chen Hsiung Hung,*,2 and Eric Wei-Guang Diau, Development of Hybrid Pseudohalide Tin Perovskites for Highly Stable Carbon-Electrode Solar Cells, Downloaded from pubs.acs.org/aamick/article-supplement/584575/pdf/am0c03704_si_001/ by guest on 24 August 2026.
[137] Seyedeh Mozhgan , Seyed-Talebi, Mehrnaz Mahmoudi, Chih-Hao Lee, A Comprehensive Study of CsSnI3-Based Perovskite Solar Cells with Different Hole Transporting Layers and Back Contacts Article Full-text available, Aug 2023 ,
[138] AlZoubi, T.; Kadhem, W.J.; Al Gharram, M.; Makhadmeh, G.;Abdelfattah, M.A.O.; Abuelsamen, A. AL-Diabat, A.M.; Abu Noqta, O.; Lazarevic, B.; Zyoud, S.H.; et al. Advanced Optoelectronic Modeling and Optimization of HTL-Free FASnI3/C60 Perovskite Solar Cell Architecture for Superior Performance. Nanomaterials 2024, 14, 1062. https://doi.org/10.3390/nano14121062.
[139] Seyed-Talebi, S.M.; Mahmoudi, M.; Lee, C.-H., A Comprehensive Study of CsSnI3-Based Perovskite Solar Cells with Different Hole Transporting Layers and Back Contacts. Micromachines 2023, 14, 1562. https://doi.org/10.3390/mi14081562.
[140] M. Khalid Hossain,* G. F. Ishraque Toki, D. P. Samajdar,* Muhammad Mushtaq, M. H. K. Rubel,* Rahul Pandey,* Jaya Madan, Mustafa K. A. Mohammed, Md. Rasidul Islam, Md. Ferdous Rahman, and H. Bencherif, Deep Insights into the Coupled Optoelectronic and Photovoltaic Analysis of Lead-Free CsSnI3 Perovskite-Based Solar Cell Using DFT Calculations and SCAPS-1D Simulations, ACS Omega 2023, 8, 22466−22485, http://pubs.acs.org/journal/acsodf.
[141] Park, H.-J.; Son, H.; Jeong,B.-S. SCAPS-1D Simulation for Device Optimization to Improve Efficiency in Lead-Free CsSnI3 Perovskite Solar Cells. Inorganics 2024, 12, 123. https://doi.org/10.3390/inorganics12040123.
[142] Eli Danladi a,*, Philibus M. Gyuk b, Nicholas N. Tasie c, Anselem C. Egbugha d,Debidatta Behera e, Ismail Hossain f, Ibrahim M. Bagudo g, Mohammad L. Madugu h, Jonathan T. Ikyumbur, Impact of hole transport material on perovskite solar cells with different metal electrode: A SCAPS-1D simulation insight, https://doi.org/10.1016/j.heliyon.2023.e16838.
[143] Nejmeddine Yahyaoui, Multiscale Modeling of Quantum Dot Solar Cells: Integration of Density Functional Theory, SCAPS, Lambert W Analysis, and Machine Learning, ACS Omega 2026, 11, 30322−30344, https://doi.org/10.1021/acsomega.6c01622.

(This work is licensed under a Creative Commons Attribution 4.0 International License.)